Rastislav Ďuriš, Justín Murín

A Solution for 1D Non-linear Problems for Finite Elements With Full Stiffness Matrices

Scientific Monographs in Automation and Computer Science

Edited by
Prof. Dr. Peter Husar (Ilmenau University of Technology) and
Dr. Kvetoslava Resetova (Slovak University of Technology in Bratislava)

Vol. 9

A SOLUTION FOR 1D NON-LINEAR PROBLEMS FOR FINITE ELEMENTS WITH FULL STIFFNESS MATRICES

Rastislav Ďuriš

Justín Murín

Universitätsverlag Ilmenau
2012

Impressum

Bibliographic information of the German National Library
The German National Library lists this publication in the German national bibliography, with detailed bibliographic information on the Internet at http://dnb.d-nb.de.

Author's acknowledgement to Juraj Miština for translation.

This scientific monograph originated from the author's dissertation thesis defended at the Slovak University of Technology in Bratislava, Faculty of Materials Science and Technology in Trnava.

Reviewers:
Prof. Ing. Pavel Élesztös, CSc.
Prof. Dr. Ing. Vladimír Kompiš, CSc.
Prof. Ing. Milan Žmindák, CSc.

Author's contact address:
Ing. Rastislav Ďuriš, PhD.
Slovak University of Technology in Bratislava
Faculty of Materials Science and Technology in Trnava

Prof. Ing. Justín Murín, DrSc.
Slovak University of Technology in Bratislava
Faculty of Electrical Engineering and Information Technology

Ilmenau Technical University / University Library
Universitätsverlag Ilmenau
Postfach 10 05 65
98684 Ilmenau
www.tu-ilmenau.de/universitaetsverlag

Production and delivery
Verlagshaus Monsenstein und Vannerdat OHG
Am Hawerkamp 31
48155 Münster
www.mv-verlag.de

ISSN 2193-6439 (Print)
ISBN 978-3-86360-053-2 (Print)
URN urn:nbn:de:gbv:ilm1-2012100225

Titelfoto: photocase.com

Abstract

The requirements for the advanced design and production of structures with high performance, material and economic efficiency lead to the need for use of the structural elements with stiffness variation. Varying stiffness can be caused by continuous change of a cross-section and/or by using materials with varying material properties.

Structural analysis of truss and frame structures consisting of structural parts with stiffness variation can be difficult. The stiffness variation of structural parts can be modelled by applying the fine beam FE mesh or 3D solid finite elements with average values of cross-sectional and material parameters.

If classical finite elements are used, FE analyses of these structures require application of models with extremely fine mesh; thus the preparation of a computational model is very time-consumption and computational time can be too large, particularly in non-linear analyses.

For elimination of the mentioned disadvantages of classical finite element applications, a two-node non-linear bar element with varying stiffness is developed in the first part of the monograph. Concerning the bar element, the continuous longitudinal variation of cross-sectional area and material properties is considered. The stiffness matrices of the developed finite element were derived using full geometric non-linear, non-incremental formulations of equilibrium equations without any linearization for a linear elastic loading state. New shape functions derived from the modified concept of transfer functions and constants allow the accurate description of

polynomial variation of the cross-sectional area and material properties in the bar element. Further, this approach was extended to the solution of physically non-linear problems.

The matrices of non-linear bar elements were modified for the application of materials with a uni-axial, bilinear stress-strain relationship and isotropic or kinematic hardening. A non-incremental solution algorithm was formulated for geometric and physically non-linear analysis using the derived bar element matrices.

For the implementation of varying properties of the composite—sandwich and functionally graded materials (FGM) into derived stiffness matrices—the determination of effective homogenized material properties is necessary. Macro-mechanical modelling of composite material properties is based on the different homogenization techniques. In this thesis, a two-component composite with longitudinal variation of elasticity modulus and volume fractions was considered. The effective homogenized properties of the chosen composite were calculated using the new extended mixture rule formulated at the Department of Mechanics of the Faculty of Electrical Engineering and Information Technology, Slovak University of Technology in Bratislava, Slovakia. The homogenization of thermo-mechanical material properties was carried out for multilayers sandwich bars with polynomial variation of the effective Young's modulus and volume fractions of fibre and matrix in the layers. The procedure for including the varying temperature field by means of thermal nodal forces was developed as well. The normal stress distribution in composite layers of the original non-

homogenized sandwich bar was calculated by effective computational method.

In the second part of the thesis, the stiffness matrices of a geometrically non-linear beam finite element were derived using a full non-linear, non-incremental formulation without any linearization. The matrices of the two-node plane beam element with a double-symmetric cross-section and constant stiffness were formulated.

The suitability of the concept of transfer constants implementation, the accuracy and efficiency of a geometrically and physically non-linear bar element, a geometrically non-linear beam finite element, and applicability of the extended mixture rule were compared and assessed by several numerical experiments against ANSYS analyses with classical finite elements. A good agreement between results obtained by newly developed elements and the reference solutions in the commercial FEM code ANSYS was achieved. Moreover, the high efficiency of the developed procedures was proved.

Key words

geometric non-linear problems, finite elements, stiffness matrix, plasticity bar element, beam element

List of abbreviations and symbols

TLF	total Lagrange formulation
ULF	updated Lagrange formulation
GLT	Green-Lagrange strain tensor
LCS	local coordinate system
GCS	global coordinate system
II.PKT	second Piola-Kirchhoff stress tensor
E_{ij}	Green-Lagrange strain tensor
e_{ij}	linear part of Green-Lagrange strain tensor
η_{ij}	non-linear part of Green-Lagrange strain tensor
S_{ij}	second Piola-Kirchhoff stress tensor
q_k	local nodal displacement (rotation)
u_i	global nodal displacement (rotation)
ϕ_{ij}	shape function
$\mathbf{C}$	tensor of elastic material properties
$\mathbf{F}$, $\mathbf{F}^{ext}$	vector of local external nodal forces
$\mathbf{F}^{int}$	vector of local internal nodal forces
$\mathbf{F}^{Gext}$	vector of global external nodal forces
$\mathbf{F}^{Gint}$	vector of global internal nodal forces
$\mathbf{q}$	vector of local nodal displacements
$\mathbf{K}$	local stiffness matrix in the invariant form
$\mathbf{K}(\mathbf{q})$	local stiffness matrix as function of nodal displacement
$\mathbf{K}^T$	local tangent stiffness matrix in the invariant form

$\mathbf{K}^T(\mathbf{q})$ local tangent stiffness matrix with displacement dependent elements

$\mathbf{N}$ shape function matrix

$\mathbf{T}$; $\mathbf{T}^{\mathrm{T}}$ transformation matrix; transposed transformation matrix

$\boldsymbol{\varepsilon}_0$ strain vector induced temperature field

A^0 cross-sectional area in initial configuration (undeformed)

$A(x)$ continuously variable cross-sectional area (undeformed)

E elasticity modulus (Young's modulus)

E_f elasticity modulus of fibres

E_m elasticity modulus of matrix

$E(x)$ elasticity modulus continuously varied along the longitudinal axis of the element

E_T tangent modulus

$E_f(x)$ elasticity modulus of fibres continuously varied along the longitudinal axis of the element

$E_m(x)$ elasticity modulus of matrix continuously varied along the longitudinal axis of the element

$E_T(x)$ tangent modulus continuously variable along the longitudinal axis of the element

$E_L^H(x)$ effective homogenized elasticity modulus continuously variable along the longitudinal axis of the element

$E_L(x)$ effective longitudinal variable elasticity modulus of composite material

$E_L^k(x)$ effective longitudinal variable elasticity modulus of k^{th} composite layer

I_Z second moment of area (second moment of inertia)

I_{Z2} third moment of area

I_{Z3} bi-quadratic moment of area

L^0 element length in initial (undeformed) configuration

L^t element length in current (deformed) configuration

L length of the line connecting element end nodes in the deformed state

$v_f(x)$ polynomial describing the change of fibre volume ratio

$v_m(x)$ polynomial describing the change of matrix volume ratio

V^0 body volume in initial configuration

α^0 initial angle between r axis of local coordinate system and x axis of global coordinate system

$\alpha_T(x)$ thermal expansion coefficient continuously varied along the longitudinal axis of the element

$\alpha_{TL}^H(x)$ effective homogenized thermal expansion coefficient continuously varied along the longitudinal axis of the element

$\alpha_{TL}(x)$ effective longitudinal variable thermal expansion coefficient of composite material

$\alpha_{TL}^k(x)$ effective longitudinal variable thermal expansion coefficient of k^{th} composite layer

β total rotation angle connector of element end points

λ stretching

λ_{σ_y} stretching on yield stress

ρ material density

σ_y yield stress, "mean" yield stress

$\sigma_y(x)$ yield stress continuously varied along the longitudinal axis of the element

$^{\mathrm{T}}$	right superscript $^{\mathrm{T}}$ denotes matrix transpose operation of matrix/vector
^{T}	right superscript ^{T} denotes tangent matrix
$^{(i)}$	right superscript $^{(i)}$ denotes i^{th} iteration

INTRODUCTION

If the relationship between the displacement of the body points and the external load is not linear, we are talking about the non-linear behaviour of the body. The equations necessary to describe the process of the material behaviour must include the body movement kinematics (description of the deformation process by the vector field of displacements, deformation tensors), kinetics (continuum kinetic equations, stress tensor and its increment), thermodynamics and constitutive equations (generalized Hooke's law, the relationships between stress increment and deformation in elastic-plastic loading area). Based on the kinematics of the deformation process and the used constitutive relations, non-linear behaviour of the body can be caused by physical (material) non-linearity, geometric non-linearity and mutual contact of the bodies.

Physical non-linearity occurs when the correlation between the load and deformation is not linear, e.g. if the stress in the body exceeds the limit of proportionality, which is associated with the emergence of plastic deformation or due to creep of the material.

Geometric non-linearities lead to changes in the body configuration due to the load, and the displacements of u_i points of the body and their gradient $u_{i,j}$ are no longer infinitely small but finite. The term 'finite deformations' means a complex of the body's rigid motion and strain. According to the extent of displacements of body points and the components of strain, we distinguish:

- Theory of the 1st rank comprising the area of infinitely small displacements and strains. The total strain can be additively divided into elastic and plastic components.
- Theory of the 2nd rank comprising the area of finite displacements and small strains. The additive division of the strain into elastic and plastic elements is possible.
- Theory of the 3rd rank, comprising
  a) small displacements and large strains, where the elastic element of the strain is infinitely small and the plastic element is finite. The additive division of the deformation tensor into elastic and plastic elements is acceptable after the modification of the constitutive relations,
  b) both large displacements and large strains. The additive division of the deformation tensor into elastic and plastic elements is not possible. For this case, multiplicative division is used (73).

The first part of monograph focuses on the derivation of the stiffness matrices of geometrically non-linear bar elements with variable stiffness. The second part is devoted to the derivation of the stiffness matrices of geometrically non-linear beam element with constant stiffness.

1. NON-INCREMENTAL FORMULATION FOR SOLVING GEOMETRICALLY NON-LINEAR PROBLEMS

1.1 An overview of the current state of knowledge

Numerous papers using different approaches have been published on solutions for non-linear tasks when displacements affect the structural stiffness. Among the most important studies are (5, 8, 14, 78).

The solution of geometrically non-linear problems published in (5) is based on an incremental formulation. In the derivation of the stiffness relations, the increment variation GLT is linearized (its non-linear component is neglected) and at the same time, the increment II.PKT is linearized, too. The solution procedure and derivation of the element stiffness matrices is possible by the Total Lagrange Formulation (TLF) (when all static and kinematic variables are related to initial, undeformed configuration of the body), or using the Updated Lagrange Formulation (ULF) (when all static and kinematic variables are related to the last known body configuration).

It is known that the accuracy of the results using these elements in non-linear problems depends on the mesh density. However, coarse mesh can give convergent results. The discrepancy between the calculated values and the reality is usually significant. In addition to the choice of the shape function representation, the linearization of non-linear expressions of the finite element method is the main reason for achieving inaccurate

solutions and increasing the number of iterations to achieve a balance of internal and external forces.

Another approach published in (14, 15) is based on neglected terms of higher order in variations of the increment of the Green-Lagrange deformation tensor (GLT).

To eliminate the inaccuracy caused by the linearized incremental non-linear FEM equations, a non-incremental formulation of non-linear equilibrium equations without linearization was established (42). The obtained equations contain the full non-linear stiffness matrices.

1.2 Non-incremental formulation of solving geometrically non-linear problems without linearization for the elastic zone of loading and a bar of constant cross section

In order to minimize the negative impact of linearization in the incremental formulation of equations to derive the stiffness matrices, the non-linearized non-incremental formulation was derived (42, 47).

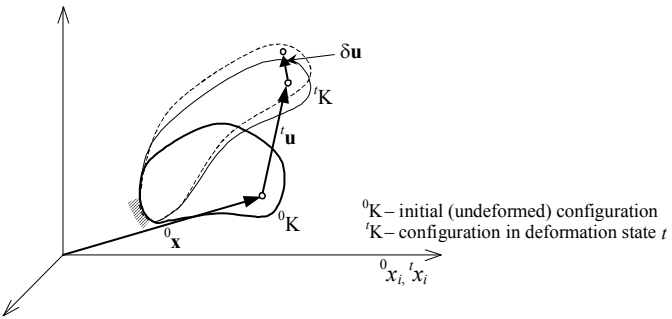

Fig. 1 *Deformation state of the body – non-incremental method*

Fig. 1 shows the deformation state of the body. Unlike the incremental formulation, in the derivation there is omitted the inter-configuration of the body in deformation step $t + \Delta t$. Upon the principle of virtual work, the static balance of the body in its immediate position ${}^{t}K$ (see Fig. 1) can be derived from equality of virtual work of internal and external forces (the Generalized Lagrange Formulation - GLF)

$$\int_{V^0} S_{ij}\,\delta E_{ij}\,dV = \int_{A^0} F_i\,\delta u_i\,dA + \vec{F}_k\,\delta q_k \ , \qquad [1.1]$$

where the integral on the left side of the equation represents the virtual work of internal forces and the expression on the right side the virtual work of external forces (only surface and concentrated to the node). The integration is performed over the initial volume V^0 (surface A^0) of the body. If for the description of the deformation process we use GLF, the deformation state of the individual points of the body will be described by the GLT of finite deformations

$$E_{ij} = e_{ij} + \eta_{ij} = \tfrac{1}{2}(u_{i,j} + u_{j,i}) + \tfrac{1}{2} u_{k,i}\, u_{k,j} \qquad [1.2]$$

Its variation is expressed fully without linearization

$$\delta E_{ij} = \delta e_{ij} + \delta \eta_{ij} \ . \qquad [1.3]$$

Using the decomposition [1.2], non-linear equilibrium equations in the current deformed configuration in non-incremental form can be expressed in the modified relation (30, 42, 49)

$$\int_{V^0} C_{ijkl}\, e_{kl}\, \delta e_{ij}\, dV + \int_{V^0} C_{ijkl}(\eta_{kl}\, \delta e_{ij} + e_{kl}\, \delta \eta_{ij} + \eta_{kl}\, \delta \eta_{ij})dV = \\ = \int_{A^0} F_i\, \delta u_i\, dA + \vec{F}_k\, \delta q_k \qquad [1.4]$$

where C_{ijkl} is the tensor of material properties defining the constitutive relation between II. Piola-Kirchhoff stress tensor $S_{ij} = C_{ijkl}\, E_{rs}$ in configuration ${}^tK$ and the Green-Lagrange strain tensor E_{ij} [1.2]. Furthermore, $u_{i,j}$ is the current deformation gradient, δu_i is a variation of displacement, F_i are the surface tractions and δq_k are virtual displacements of points of the body in which the concentrated forces $\vec{F}_k$ operate. The integration is performed through the initial (undeformed) volume V^0 and the initial area A^0 of the finite element.

By discretization of the body into finite elements, the displacement of an arbitrary point of u_i element can be expressed by interpolation of the nodal point displacements q_k of the element using shape functions ϕ_{ik}

$$u_i = \phi_{ik}\, q_k \qquad [1.5]$$

After substituting the shape functions and their derivation into the equation [1.4] and after necessary adjustments, substitution of indices and exclusion of variation δu_i to get a steady relationship describing the non-linear dependence between the displacements of points of the body and the external load, from which it is possible to derive the shape of the

stiffness matrices, valid for an arbitrary type of element, the displacements of which can be described by the expression [1.5] (30)

$$\begin{aligned}
&\frac{1}{4}\int_{V^0} C_{ijkl}(\phi_{km,l}+\phi_{lm,k})(\phi_{in,j}+\phi_{jn,i})q_m\,dV + \\
&\frac{1}{4}\int_{V^0} C_{ijkl}\,\phi_{pm,k}\,\phi_{pr,l}(\phi_{in,j}+\phi_{jn,i})q_m\,q_r\,dV + \\
&\frac{1}{2}\int_{V^0} C_{ijkl}\,\phi_{pr,i}\,\phi_{pn,j}(\phi_{km,l}+\phi_{lm,k})q_m\,q_r\,dV + \\
&\frac{1}{2}\int_{V^0} C_{ijkl}\,\phi_{pm,k}\,\phi_{pv,l}\,\phi_{rq,i}\,\phi_{rn,j}\,q_m\,q_v\,q_q\,dV = \int_{A^0} F_i\,\phi_{in}\,dA + \vec{F}_n\,.
\end{aligned} \qquad [1.6]$$

Equation [1.6] can be rewritten for a single element into component K_{nm} $q_m = F_n$, or in matrix form

$$\mathbf{K}(\mathbf{q})\,\mathbf{q} = \mathbf{F}\,, \qquad [1.7]$$

The local non-linear stiffness matrix consists of one linear and three non-linear components

$$\mathbf{K}(\mathbf{q}) = \mathbf{K}^L + \mathbf{K}^{NL1}(\mathbf{q}) + \mathbf{K}^{NL2}(\mathbf{q}) + \mathbf{K}^{NL3}(\mathbf{q}) = \mathbf{K}^L + \mathbf{K}^{NL}(\mathbf{q}) \qquad [1.8]$$

Terms of the nonlinear stiffness matrix $\mathbf{K}^{NL}(\mathbf{q})$ depend on the local nodal displacement vector $\mathbf{q}$ in the form of linear and quadratic functions.

The system of non-linear equations [1.7] has to be solved by one of the iterative methods. In case of Newton's (or Newton-Rapson) iterative scheme, to achieve a better rate of convergence of solution, it is necessary

to compile a tangential stiffness matrix $\mathbf{K}^T(\mathbf{q})$ of the element according to the following procedure:

$$\mathbf{K}^T(\mathbf{q}) = \frac{\partial \mathbf{F}}{\partial \mathbf{q}} = \mathbf{K}(\mathbf{q}) + \frac{\partial \mathbf{K}(\mathbf{q})}{\partial \mathbf{q}}\mathbf{q} = \mathbf{K}^L + \mathbf{K}^{NLT}(\mathbf{q}) \ , \qquad [1.9]$$

where $\mathbf{K}^{NLT}(\mathbf{q})$ is non-linear part of the tangential stiffness matrix $\mathbf{K}^T(\mathbf{q})$.

2. BAR ELEMENT WITH VARIABLE STIFFNESS FOR SOLVING GEOMETRICALLY AND PHYSICALLY NONLINEAR PROBLEMS

At present, we encounter in technical practice the use of mechanical parts with variable stiffness, either due to economic and technological reasons, or because of the use of new advanced materials such as composites and sandwich structures or Functionally Graded Materials (FGM).

When modelling the bar and frame structures, the problem of stiffness variability can be reduced by using "average" values of the section and material properties, by choice of the greater density of network elements with differentiation of section and material properties, or by modelling the parts of structures with variable stiffness by planar or solid finite elements. However, apart from the increase of time required to prepare the model and the solution itself, it adds the problem with inter-element compatibility.

Therefore, based on the results obtained in numerical experiments, which confirm the accuracy and efficiency of the new, geometrically non-linear bar element with constant stiffness loaded in the area of elastic deformations, this solution was extended to allow for continuous variation of the cross-sectional area and material properties. Further, the solution was also extended to solve the physical non-linear problems and the possibility to apply the temperature field with a prescribed temperature distribution along the longitudinal axis of the bar as the load to the element was applied. This procedure aims to regard the continuous variation of the bar stiffness using a single bar element without having to create a relatively dense network of finite elements.

2.1 Geometrically non-linear elastic bar element with variable stiffness

2.1.1 Defining the variability of input parameters

In order to meet and describe the continuous variation of the cross-sectional area and material properties along the longitudinal axis of the one-dimensional element in the derivation stiffness relationship, the concept of transfer functions and constants published by H. Rubin in (69) and extended by J. Murín and V. Kutiš (30, 46, 47, 51) was used. This leads to the establishment of new shape functions interpolating displacement of an arbitrary point of the element from the displacements of the bar element nodal points. New shape functions include the so-called transfer functions, their derivatives and transfer constants (values of shape functions in the terminal node of element). Using this approach is conditioned by the description variability of cross-sectional characteristics and material properties in the polynomial shape. We can assume that the continuous variation of the cross-sectional area $A(x)$ or elastic modulus $E(x)$ in the axis of the element can be described by the polynomial in the form

$$P(x) = P_i \, \eta_P(x) = P_i \left(1 + \sum_{k=1}^{n} \eta_{Pk} x^k \right) \qquad [2.1]$$

where η_{Pk} are the coefficients of polynomial members $\eta_P(x)$ describing the variability of mechanical or geometric parameter, and P_i is the size of the variable is the initial node i of the element.

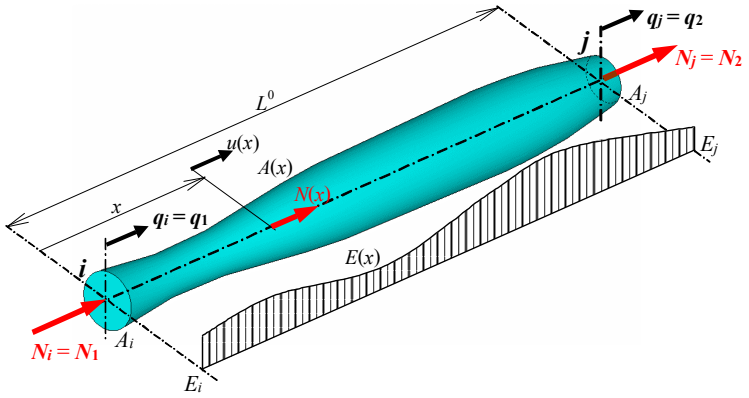

Fig. 2 *Bar with variable stiffness for solving of elastic problems*

Then the variability of elastic axial stiffness can be expressed in the relationship

$$A(x)\,E(x) = A_i\,E_i\,\eta_E(x)\,\eta_A(x) = A_i\,E_i\,\eta_{AE}(x) \qquad [2.2]$$

where $\eta_{AE}(x) = A(x)\,E(x)/A_i\,E_i$ is the polynomial describing stiffness variation along the longitudinal axis of the bar.

2.1.2 New shape functions of the two-node bar element

The kinematic relationship between the axial displacement at the location x of an arbitrary point of element $u(x)$ and axial force $N(x)$ in place x is expressed by the differential equation

$$u'(x) = \frac{du(x)}{dx} = \frac{N(x)}{A(x)\,E(x)} = \frac{N(x)}{A_i\,E_i}\,d''_{2e}(x) \qquad [2.3]$$

We can define the second derivative of the transfer function $d_{2e}(x)$ for the tension/compression loading in the linear elastic loading area (subscript *e*) as

$$d''_{2e}(x) = \frac{d^2(d_{2e}(x))}{dx^2} = \frac{1}{\eta_{AE}(x)} \qquad [2.4]$$

Then the solution of differential equations [2.3], provided that all the loads of the element are transformed into nodes of the element and the axial force in the bar is constant ($N(x) = -N_i = N_j$), the function describing the axial displacement of any point of the element is

$$u(x) = q_i - \frac{N_i}{A_i E_i}\,d'_{2e}(x) \qquad [2.5]$$

where $d'_{2e}(x)$ is the first derivation of transfer function, for which is valid

$$d'_{2e}(x) = \int_0^x \frac{1}{\eta_{AE}(x)}\,dx\ .$$

By substitution of $x = L^0$ in equation [2.5] the displacement is $u(L^0) = q_j$, and $d'_{2e}(L^0) = d'_{2e}$ indicates the value of the first derivative of the transfer function in the terminal node of the element and will be further called the transfer constant for tension/compression. Calculation of the transfer constant d'_{2e} can be done numerically using a simple algorithm, published in (30, 53). By deriving an axial force N_i z from this way modified equation, and by backward substitution into equation [2.5] we obtain the dependence

between the axial displacement of an arbitrary point of the bar in the direction of the x-axis and the axial displacement of nodal points i and j, expressed by the new shape functions $\phi(x)$

$$u(x) = \left(1 - \frac{d'_{2e}(x)}{d'_{2e}}\right) q_i + \frac{d'_{2e}(x)}{d'_{2e}} q_j = \phi_{ui}(x)\, q_i + \phi_{uj}(x)\, q_j \qquad [2.6]$$

The first derivatives of the shape functions for two-node bar element with varying stiffness are then equal to

$$\phi_{11,1}(x) = -\frac{d''_{2e}(x)}{d'_{2e}} \quad , \quad \phi_{12,1}(x) = \frac{d''_{2e}(x)}{d'_{2e}} \quad . \qquad [2.7]$$

2.1.3 Local non-linear stiffness matrix of bar element with variable stiffness

By substituting the derivatives of shape functions [2.7] for the two-node bar element and by the substitution for the one-dimensional element $dV = A(x)\, dx = A_i \eta_A(x) dx$ and for the tensor of elastic behaviour of the material $C_{ijkl}(x) \equiv E(x) = E_i \eta_E(x)$ into the first integral in equation [1.6], we obtain an expression for the calculation of the linear members of the stiffness matrix bar element with variable stiffness:

$$K^L_{nm} = A_i E_i \int_{L^0} \eta_{AE}(x) \phi_{1m,1}(x) \phi_{1n,1}(x)\, dx \quad . \qquad [2.8]$$

Using the same procedure we get members of the non-linear stiffness matrices (dependent on the unknown displacements of terminal nodes of the

bar element) by the substitution and modification of other members in the equation [1.6]:

$$K_{nm}^{NL1} = \frac{1}{4} A_i E_i \int_{L^0} \eta_{AE}(x) \phi_{1m,1}(x) \left(\phi_{11,1}(x) q_1 + \phi_{12,1}(x) q_2\right) 2\phi_{1n,1}(x)\, dx \qquad [2.9]$$

$$K_{nm}^{NL2} = \frac{1}{2} A_i E_i \int_{L^0} \eta_{AE}(x) \phi_{1n,1}(x) \left(\phi_{11,1}(x) q_1 + \phi_{12,1}(x) q_2\right) 2\phi_{1m,1}(x)\, dx \qquad [2.10]$$

$$K_{nm}^{NL3} = \frac{1}{2} A_i E_i \int_{L^0} \eta_{AE}(x) \left(\phi_{11,1}(x) q_1 + \phi_{12,1}(x) q_2\right)^2 \phi_{1m,1}(x) \phi_{1n,1}(x)\, dx \qquad [2.11]$$

Substituting derivatives of shape functions [2.7] into equations [2.9] and [2.10] results in the need for calculation of the integrals $\int_{L^0} (d''_{2e}(x))^2 dx$ and $\int_{L^0} (d''_{2e}(x))^3 dx$. By substitution of integrants, where in the denominator of the relation [2.4] we replace the polynomial $\eta_{AE}(x)$ for $(\eta_{AE}(x))^2 = \bar{\eta}_{AE}(x)$ or $(\eta_{AE}(x))^3 = \bar{\bar{\eta}}_{AE}(x)$ entails the need for the calculation of integrals $\int_{L^0} \frac{1}{\bar{\eta}_{EA}(x)} dx = \overline{d_{2e}}$ and $\int_{L^0} \frac{1}{\bar{\bar{\eta}}_{EA}(x)} dx = \overline{\overline{d_{2e}}}$.

This way, we get new transfer constants $\overline{d_{2e}}$ and $\overline{\overline{d_{2e}}}$ of the bar element for variable stiffness and the elastic loading area. To calculate these transfer constants, the algorithm mentioned in (32, 33, 49, 50, 51), can be used, since $\bar{\eta}_{EA}(x)$ and $\bar{\bar{\eta}}_{EA}(x)$ are also polynomials. The final shape of the local

non-linear stiffness matrix of the bar element with variable stiffness can be expressed as

$$\mathbf{K}(\mathbf{q}) = \frac{A_i E_i}{d'_{2e}} \left[1 + \frac{3}{2}(q_2 - q_1)\frac{\overline{d_{2e}}}{(d'_{2e})^2} + \frac{1}{2}(q_2 - q_1)^2 \frac{\overline{\overline{d_{2e}}}}{(d'_{2e})^3} \right] \begin{bmatrix} 1 & -1 \\ -1 & 1 \end{bmatrix}. \quad [2.12]$$

The vector of local nodal displacement of the bar is $\mathbf{q} = [q_1 \quad q_2]^{\mathrm{T}}$ and the vector of external local nodal forces $\mathbf{F} = [N_1 \quad N_2]^{\mathrm{T}}$.

2.1.4 Local non-linear tangential stiffness matrix

The system of non-linear algebraic equations is usually solved using the iterative Newton's (or Newton-Raphson) method. Using this way of solution, the local non-linear tangential stiffness matrix is required. This tangential stiffness matrix can be calculated using the relation [1.9], by derivation of matrix **K(q)** [2.12]. After the relevant derivations according to nodal displacements q_i we get the expression for the local non-linear tangential stiffness matrix of the two-node bar element with variable stiffness

$$\mathbf{K}^T(\mathbf{q}) = \frac{A_i E_i}{d'_{2e}} \left[1 + 3(q_2 - q_1)\frac{\overline{d_{2e}}}{(d'_{2e})^2} + \frac{3}{2}(q_2 - q_1)^2 \frac{\overline{\overline{d_{2e}}}}{(d'_{2e})^3} \right] \begin{bmatrix} 1 & -1 \\ -1 & 1 \end{bmatrix} \quad [2.13]$$

2.1.5 Global non-linear tangential stiffness matrix

For the calculation of the global displacements of nodal points of the bar element from the system of global non-linear equilibrium equations we use

Newton's iteration method. This procedure uses the global non-linear tangential stiffness matrix of the body to calculate the nodal displacements. Since the non-linear component of tangential stiffness [2.13] is not invariant to rigid motion of the body, for transformation between the local and the global stiffness matrix, it is not possible to use standard transformation, known from the linear theory.

Therefore, we apply replacement of nodal displacements by the value invariant to the rigid motion of the body - by stretching λ

$$\lambda = \frac{L}{L^0} = 1 + \frac{\Delta L}{L^0} = 1 + \frac{q_2 - q_1}{L^0} \ . \qquad [2.14]$$

By substituting the relation [2.14] into the relationship [2.13] we obtain invariant component of non-linear tangential stiffness in the form

$$\mathbf{K}^T = \frac{A_i E_i}{d'_{2e}} \left[1 + 3(\lambda - 1) L^0 \frac{\overline{d_{2e}}}{(d'_{2e})^2} + \frac{3}{2}(\lambda - 1)^2 (L^0)^2 \frac{\overline{\overline{d_{2e}}}}{(d'_{2e})^3} \right] \begin{bmatrix} 1 & -1 \\ -1 & 1 \end{bmatrix}. \qquad [2.15]$$

From such expressed local non-linear tangential stiffness matrix $\mathbf{K}^T$, the global non-linear tangential stiffness matrix $\mathbf{K}_G^T$ can be expressed by classical transformation using the transformation matrix $\mathbf{T}$.

2.1.6 Internal forces

In the iteration process of the solution it is necessary to compute the vector of global internal forces. The global internal forces are formulated from the local equilibrium stiffness relation [1.7], where local non-linear stiffness

matrix **K**(**q**) is defined by the formula [2.12]. Internal forces in a bar cannot be calculated from the global stiffness relationship, in relation to the impact of large rotations. Due to the elimination of the problems associated with the transformation of internal forces from the global to the local coordinate system, we rewrite the local non-linear stiffness matrix **K**(**q**) using stretching λ [2.14] into the form of local stiffness matrix **K,** invariant to the rigid motion (rotation) of the bar

$$\mathbf{K} = \frac{A_i E_i}{d'_{2e}} \left[1 + \frac{3}{2}(\lambda - 1) L^0 \frac{\overline{d_{2e}}}{(d'_{2e})^2} + \frac{1}{2}(\lambda - 1)^2 (L^0)^2 \frac{\overline{\overline{d_{2e}}}}{(d'_{2e})^3} \right] \begin{bmatrix} 1 & -1 \\ -1 & 1 \end{bmatrix}. \quad [2.16]$$

The local internal axial force can be calculated by multiplying the total non-linear stiffness of the bar and its deformation

$$N_i = -\frac{A_i E_i}{d'_{2e}} \left[1 + \frac{3}{2}(\lambda - 1) L^0 \frac{\overline{d_{2e}}}{(d'_{2e})^2} + \frac{1}{2}(\lambda - 1)^2 (L^0)^2 \frac{\overline{\overline{d_{2e}}}}{(d'_{2e})^3} \right] (\lambda - 1) L^0 \quad [2.17]$$

.

The stress in a bar can be determined from the relationship

$$\sigma = -\frac{E_i}{d'_{2E}} \left[1 + \frac{3}{2}(\lambda - 1) L^0 \frac{\overline{d'_{2E}}}{(d'_{2E})^2} + \frac{1}{2}(\lambda - 1)^2 (L^0)^2 \frac{\overline{\overline{d'_{2E}}}}{(d'_{2E})^3} \right] (\lambda - 1) L^0 \quad [2.18]$$

where $d'_{2E}, \overline{d'_{2E}}, \overline{\overline{d'_{2E}}}$ are transfer constants for variation of elastic modulus $E(x)$. They are designed by the same procedure as the transfer constants derived in Sections 2.1.2 and 2.1.3, however, based on the second derivative of the transfer function $d''_{2E}(x) = 1/\eta_E(x)$ defined only by a polynomial of

the variability of modulus of elasticity $E(x)$. The polynomial describing the variability of modulus of elasticity $\eta_E(x)$ is in accordance with equation [2.1]. The local internal force vector is in the form $\mathbf{F}^{\text{int}} = \begin{bmatrix} N_i & N_j \end{bmatrix}^{\text{T}} = \begin{bmatrix} N_i & -N_i \end{bmatrix}^{\text{T}}$.

2.2 Geometrically non-linear bar element stressed in the elasto-plastic area

2.2.1 Defining the variability of input parameters

Let us consider the direct two-node bar element with variable stiffness, loaded in the elasto-plastic area (Fig. 3). Variability of material properties is extended in the continuous variation of elastic-plastic modulus $E_T(x)$ and yield strength $\sigma_y(x)$ along the longitudinal axis of the bar. Variability of cross-section $A(x)$ and the modulus of elasticity $E(x)$ is defined in accordance with the polynomial [2.1]. Tangent modulus $E_T(x)$ is defined by a similar polynomial. Then, the elasto-plastic stiffness variation along the longitudinal axis of the bar in the loading area above the yield strength can be expressed by expression similar to the equation [2.2]

$$A(x)E_T(x) = A_i E_{Ti} \eta_A(x)\eta_{E_T}(x) = A_i E_{Ti} \eta_{AE_T}(x) \qquad [2.19]$$

In further solution, we will deal only with material models described by bilinear stress-strain diagram with isotropic or kinematic hardening.

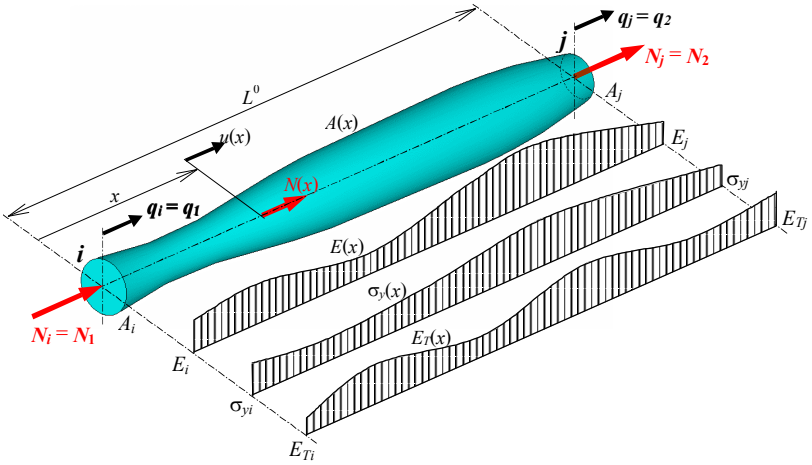

Fig. 3 *Bar with variable stiffness for solving of elasto-plastic problems*

In the case of variability of the modulus of elasticity $E(x)$ and tangent modulus of elasticity $E_T(x)$, the plastic modulus $H = \dfrac{E\,E_T}{E - E_T}$ would not have polynomial shape required for application of the concept of transfer functions and constants (69). Therefore it would be necessary to approximate the change in the plastic modulus H using the Taylor series to the polynomial shape.

2.2.2 Modification of the stiffness matrix for non-incremental solution

If the normal stress in a bar exceeds the yield stress of material σ_y, it is necessary to set up a new dependence between stress increment and relative deformation in the bar.

With preserving non-incremental solution also in the area of elasto-plastic stress, after reaching the state of plasticity in the bar, the elastic stiffness of the bar k_e will be changed into the elasto-plastic stiffness. The local stiffness matrix of the elasto-plastic stiffness of the bar will have the form

$$\mathbf{K}_{ep} = \frac{A_i E_{Ti}}{d'_{2ep}} \left[1 + \frac{3}{2}(\lambda - \lambda_{\sigma_y}) L^0 \frac{\overline{d'_{2ep}}}{(d'_{2ep})^2} + \frac{1}{2}(\lambda - \lambda_{\sigma_y})^2 (L^0)^2 \frac{\overline{\overline{d'_{2ep}}}}{(d'_{2ep})^3} \right] \begin{bmatrix} 1 & -1 \\ -1 & 1 \end{bmatrix} \quad [2.20]$$

where expression $(\lambda - \lambda_{\sigma_y})$ represents the size of elasto-plastic relative deformation of the bar $\varepsilon_{ep} = \varepsilon - \varepsilon_{\sigma_y}$ above the yield stress, expressed with the help of stretching [2.14]. Parameter λ_{σ_y} indicates stretching in the bar at reaching the yield stress and is derived from the solution of cubic equation

$$\frac{(L^0)^3}{2} \frac{\overline{\overline{d'_{2e}}}}{(d'_{2e})^4} (\lambda_{\sigma_y} - 1)^3 + \frac{3(L^0)^2}{2} \frac{\overline{d'_{2e}}}{(d'_{2e})^3} (\lambda_{\sigma_y} - 1)^2 + \frac{L^0}{d'_{2e}} (\lambda_{\sigma_y} - 1) + \frac{\sigma_y}{E_i} = 0 \quad [2.21]$$

e.g. by factorisation, where σ_y is the "mean" value of the yield stress of material of the bar

$$\sigma_y = \frac{\sigma_{yi}}{L^0} \int_0^{L^0} \eta_{\sigma_y}(x)\, dx \quad [2.22]$$

where σ_{yi} is the value of yield stress in the initial node *i* of the element and $\eta_{\sigma_y}(x)$ is the polynomial describing the variability of yield stress along the length of the element. The transfer constants $d'_{2ep}, \overline{d'_{2ep}}, \overline{\overline{d'_{2ep}}}$ are constants for elasto-plastic stress condition. These transfer constants can be determined in a similar way as the transfer constants for the case of elastic

loading (see subsections 2.1.2 and 2.1.3). The difference is only in the definition of the square derivative of the transfer function, which in this case has the form $d''_{2ep}(x) = 1/\eta_{AE_T}(x)$ defined by the polynomial of variability of elasto-plastic bar stiffness $A(x)E_T(x)$. The polynomial describing variability of elasto-plastic bar stiffness $\eta_{AE_T}(x)$ above the yield stress is defined by the equation [2.19].

2.2.3 Internal force in the bar, stress in the bar

Internal force in the bar element under the stress in elastic area is calculated from equation [2.17]. The force in the rod when reaching yield stress is equal to

$$N_{i\sigma_y} = -\frac{A_i E_i}{d'_{2e}}\left[1+\frac{3}{2}(\lambda_{\sigma_y}-1)L^0\frac{\overline{d'_{2e}}}{(d'_{2e})^2}+\frac{1}{2}(\lambda_{\sigma_y}-1)^2(L^0)^2\frac{\overline{\overline{d'_{2e}}}}{(d'_{2e})^3}\right](\lambda_{\sigma_y}-1)L^0 \quad [2.23]$$

and elasto-plastic component of axial force is expressed by the relation

$$N_{iep} = -\frac{A_i E_{Ti}}{d'_{2ep}}\left[1+\frac{3}{2}(\lambda-\lambda_{\sigma_y})L^0\frac{\overline{d'_{2ep}}}{(d'_{2ep})^2}+\frac{1}{2}(\lambda-\lambda_{\sigma_y})^2(L^0)^2\frac{\overline{\overline{d'_{2ep}}}}{(d'_{2ep})^3}\right](\lambda-\lambda_{\sigma_y})L^0 \quad [2.24]$$

The total force in the bar in elasto-plastic state is given by the sum of $N_i = N_{i\sigma_y} + N_{iep}$. The total normal stress in the bar in elasto-plastic state can be calculated by the sum of elasto-plastic stress increment σ_{ep} above the yield stress and the "mean" value of yield stress σ_y [2.22], which can be expressed by the relationship

$$\sigma = -\frac{E_{Ti}}{d'_{2E_T}}\left[1+\frac{3}{2}(\lambda-\lambda_{\sigma_y})L^0\frac{\overline{d'_{2E_T}}}{(d'_{2E_T})^2}+\frac{1}{2}(\lambda-\lambda_{\sigma_y})^2(L^0)^2\frac{\overline{\overline{d'_{2E_T}}}}{(d'_{2E_T})^3}\right](\lambda-\lambda_{\sigma_y})L^0+\sigma_y \qquad [2.25]$$

where $d'_{2E_T}, \overline{d'_{2E_T}}, \overline{\overline{d'_{2E_T}}}$ are the transfer constants for variability elasto-plastic modulus $E_T(x)$. They are determined by the same procedure as the transfer constants derived in subsections 2.1.2 and 2.1.3, but based on the square derivative of the transfer function $d''_{2E_T}(x) = 1/\eta_{E_T}(x)$ defined only by the polynomial of variability of tangential modulus $E_T(x)$.

2.2.4 Local tangential elasto-plastic stiffness matrix

The stiffness matrix $\mathbf{K}^T$ of the elastic area, expressed by equation [2.15], in the elasto-plastic state will change to

$$\mathbf{K}^T_{ep} = \frac{A_i E_{Ti}}{d'_{2ep}}\left[1+3(\lambda-\lambda_{\sigma_y})L^0\frac{\overline{d'_{2ep}}}{(d'_{2ep})^2}+\frac{3}{2}(\lambda-\lambda_{\sigma_y})^2(L^0)^2\frac{\overline{\overline{d'_{2ep}}}}{(d'_{2ep})^3}\right]\begin{bmatrix}1 & -1\\ -1 & 1\end{bmatrix} \qquad [2.26]$$

2.2.5 Procedure of non-incremental solution of elasto-plastic problems

The procedure for the non-incremental solution of elasto-plastic problems is shown in the chart in Fig. 4.

1. Calculation of starting solution (displacements **Q**) from global linear stiffness equation

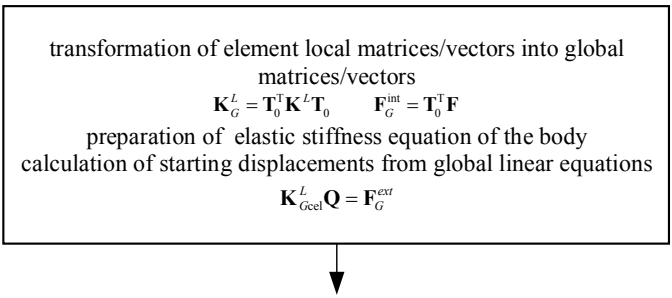

2. Preparation of global non-linear stiffness equations

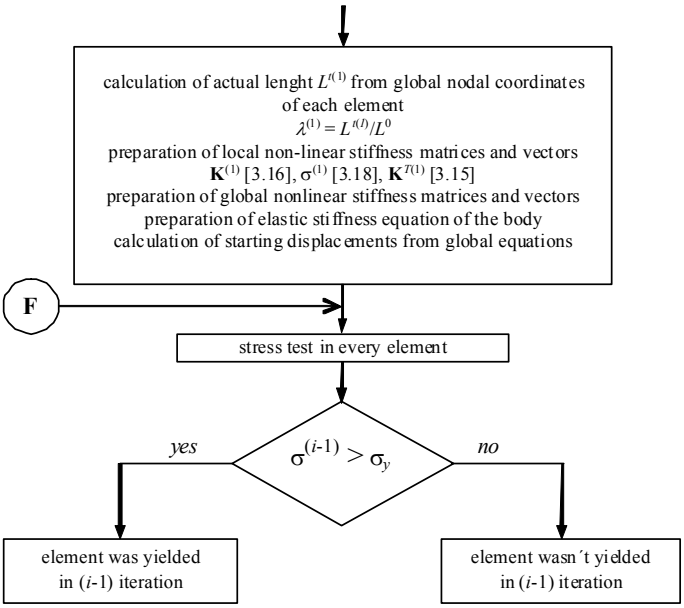

3. Evaluation of the stress status of each element

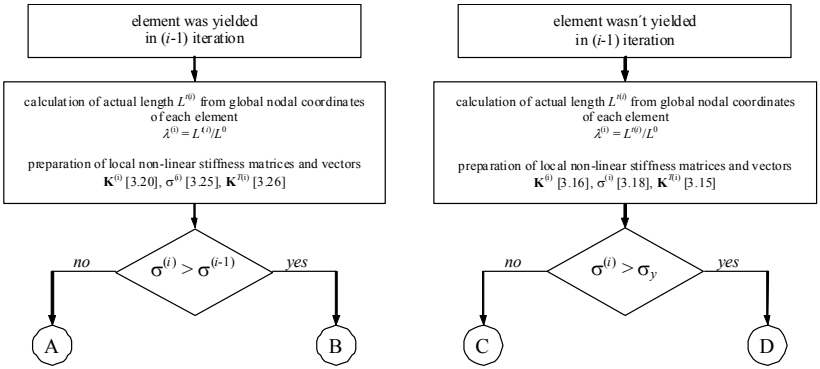

4. Calculation of axial stresses in elements and modification of stiffness matrices

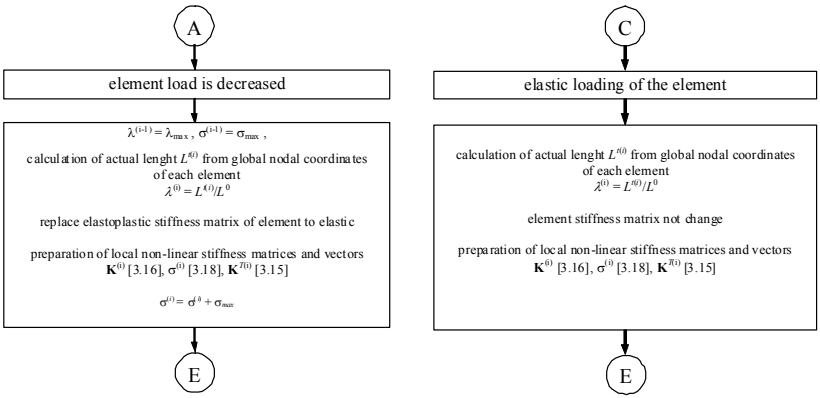

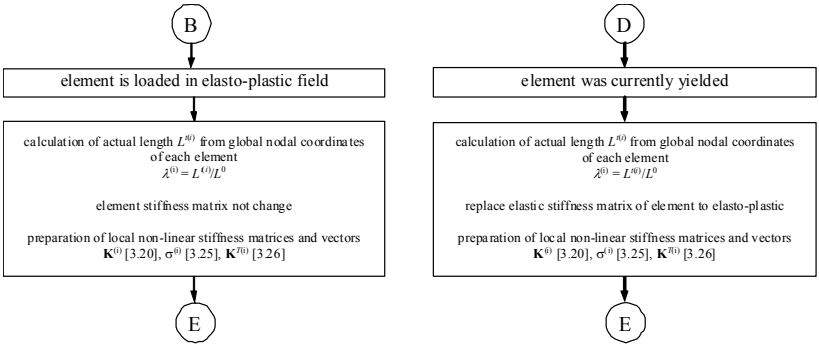

5. Preparation of new global non-linear stiffness equations, calculation of new global displacements

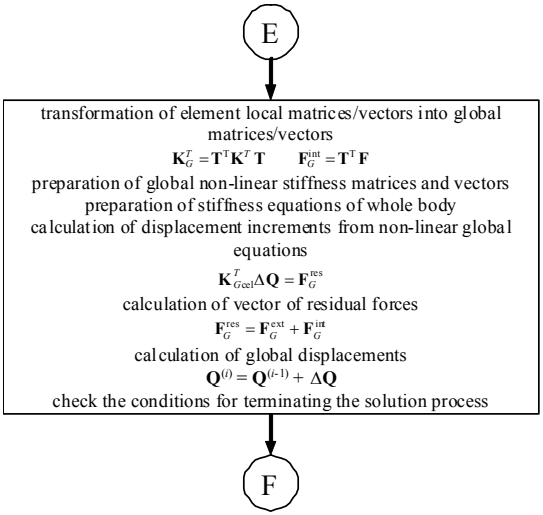

Fig. 4 *Flowchart of elasto-plastic problem solution with our bar element with variable stiffness*

2.2.6 Numerical experiments with the bar of variable stiffness loaded in elastic and elasto-plastic area

As a typical problem for studying geometrically non-linear behaviour of a structure, there was chosen a planar structure of triple joint connection of two bars, referred to in the literature as von Mises structure (Fig. 5). In the solution of the problem the small angle α^0 and symmetry of the structure were considered. Any imperfections causing a change of the straight shape of bar wasn't considered.

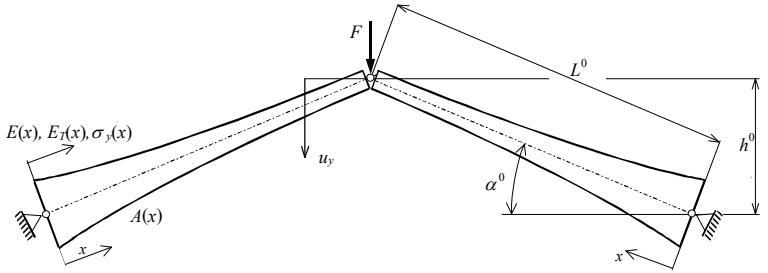

Fig. 5 *Von Mises structure with bars of variable stiffness*

Dependence between axial force in the bar N or force F and displacement of the joint node u_y, for solution in elastic area of loading and bar of constant stiffness is known for the construction according to the Fig. 6a. In the literature e.g. (5, 14), a number of approaches to analytical or numerical solutions of appointed problem can be found. The result of these solutions is the equilibrium dependence between the force in the bar of the strut frame or global reaction in the common joint, and vertical displacement of the joint, which course, when considering material with linear elastic behaviour, corresponds to the course displayed by the black line in Fig. 6c, d.

When considering loading in the elasto-plastic area, this dependence varies considerably, as is presented in Fig. 6c,d at the replacement of the diagram of tension test by the bilinear diagram with isotropic and kinematic hardening (Fig. 6b).

However, in available literature sources, any analytical solutions for the specific geometrically non-linear problem for the bar of variable stiffness and the loading in elasto-plastic area have not been found. Therefore, it was possible to assess the accuracy of the new element only by comparison with results obtained by numerical solution of the commercial finite element program ANSYS.

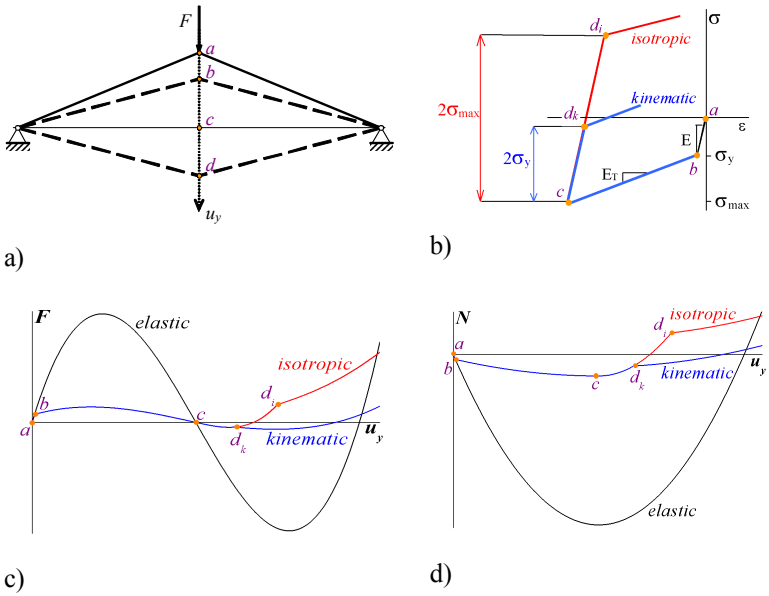

Fig. 6 *Equilibrium relationship between axial and/or global reaction and displacement of common joint for elastic and elasto-plastic material with isotropic and kinematic hardening*

2.2.6.1 Models used in the numerical experiments

To assess how accurately the stiffness matrix of the new geometrically non-linear bar element, derived in Sections 3.1 and 3.2 describe the variability of the real bar stiffness, in MATHEMATICA software are created separate programs. The programs allow solving geometrically non-linear problems under elastic and elasto-plastic loading of the new finite bar element.
In solution of all numerical experiments only one our bar element was used by procedure: *one line = one element*. The reference solutions for obtaining comparative results were created in ANSYS by simulation models:

Model BEAM23 - one-dimensional model, the element stiffness matrix is derived using Hermite shape functions. The model allows approximation of the longitudinal stiffness variation of the bar in variants with different numbers of elements. The model was designed to solve problems in elasto-plastic loading state.

Model BEAM188 - one-dimensional model using the iso-parametric beam elements BEAM188 based on the Timoshenko theory and with division into selected number of elements. The element can be used for solution of problems with large displacements (rotations) and elasto-plastic tasks.

Model SOLID45 - 3D model consisting of 2400 volume elements SOLID45. The geometric model accurately approximates the variability of the bar cross-section. Material properties were divided into 50 discrete groups, replacing the continuous variation of elasticity modulus (and tangential modulus), while values of moduli in each element were

considered to be equal to the value of the modulus in the coordinate corresponding to the centre of the element.

All the models were modelled as the direct ones, with no imperfections that would cause distortion of the straight shape of the bar model. The displacement of structure common node was prescribed within the u_y in range $\langle +L^0 \sin\alpha^0 ; -L^0 \sin\alpha^0 \rangle$ so that to obtain dependence of axial force N, or global reaction F on the displacement u_y and so the divergence solution problem near the bifurcation point was removed.

2.2.6.2 Bar with variable stiffness loaded in elasto-plastic area

We consider following initial geometric parameters of Mises structure in Fig. 5: $\alpha^0 = 7°$, $L^0 = 1$ m. Polynomials describing the variation section and material properties are listed in Table 1. The material of the bar was under consideration in the bilinear model with isotropic and kinematic hardening (Fig. 6b).

VARIATION OF CROSS-SECTIONAL AREA AND MATERIAL PROPERTIES Table 1

variation of geometric parameters and material properties [m^2, Pa]
$A(x) = 0.008 - 0.00393188x + 0.0004x^2$
$E(x) = 2\times10^{11} - 0.21154\times10^{11}x + 0.002\times10^{11}x^2$
$E_T(x) = 2\times10^{10} - 0.21154\times10^{10}x + 0.002\times10^{10}x^2$
$\sigma_y(x) = 200\times10^6 - 30\times10^6x - 10\times10^6x^2$

The maximum and minimum ratio of the bar stiffness

$$[A(x)\,E(x)]_{\max} / [\,A(x)\,E(x)]_{\min} = [A(x)\,E_T(x)]_{\max} / [\,A(x)\,E_T\,(x)]_{\min} = 2.0$$

MAXIMAL VALUES OF FORCES OBTAINED USING OUR ELEMENT AND ANSYS MODELS WITH VARIABLE STIFFNESS Table 2

	axial force N [N]		*global reaction* $\|\|F\|\|$ [N]	
No. of elem.	BEAM23	BEAM188	BEAM23	BEAM188
1	–1 878 378.92	–1 881 595.57	259 577.67	259 813.44
2	–1 829 998.74	–1 832 480.72	247 292.35	247 608.39
5	–1 817 443.47	–1 822 460.34	242 018.15	255 617.03
10	–1 815 236.23	–1 820 663.51	240 876.20	241 307.99
20	–1 815 125.26	–1 819 564.55	240 884.41	241 142.75
50	–1 815 372.23	–1 819 476.71	240 609.15	239 766.58
100	–1 814 987.56	–1 822 222.35	240 338.47	241 125.60
our element	–1 814 502.60		251 820.82	
SOLID45	–1 771 866.25		234 089.41	

Global reaction values F correspond to areas of extreme values in the first half of the course, where, as can be seen from the presented graphs, differences in the results obtained by the different models are greatest. Axial forces N in the tables correspond to the position of the bar $\alpha^t = 0°$, i.e. to the loading sub-step when the local x-axis of the bar is the same as the x-axis of the global coordinate system of the whole structure.

At the problem solution, the results were obtained using only one new non-linear bar element. As an increment of the displacement of upper node of the structure $\Delta u_y = 1$ mm was chosen, and the calculation was carried out steadily "*1 substeps = 1 iteration*."

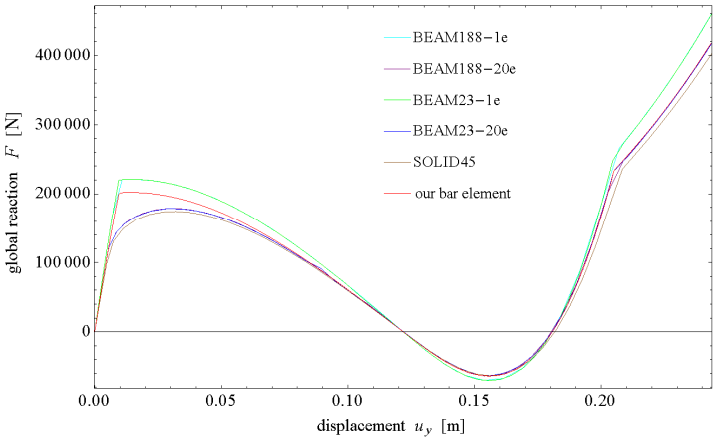

Fig. 7 *Global reaction F – common hinge displacement u_y response for the bar with isotropic hardening*

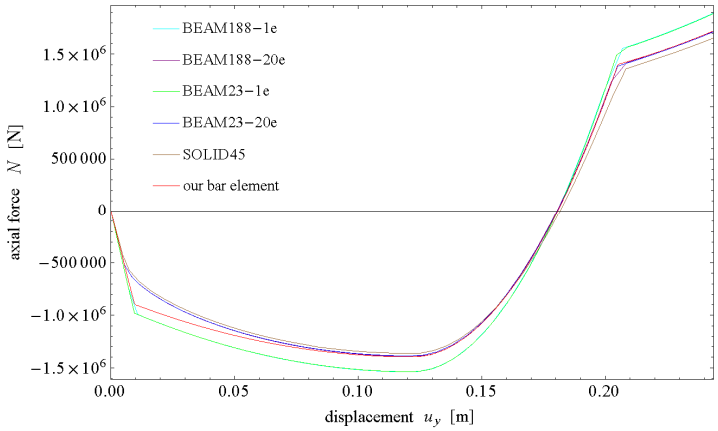

Fig. 8 *Axial force N – common hinge displacement u_y response for the bar with isotropic hardening*

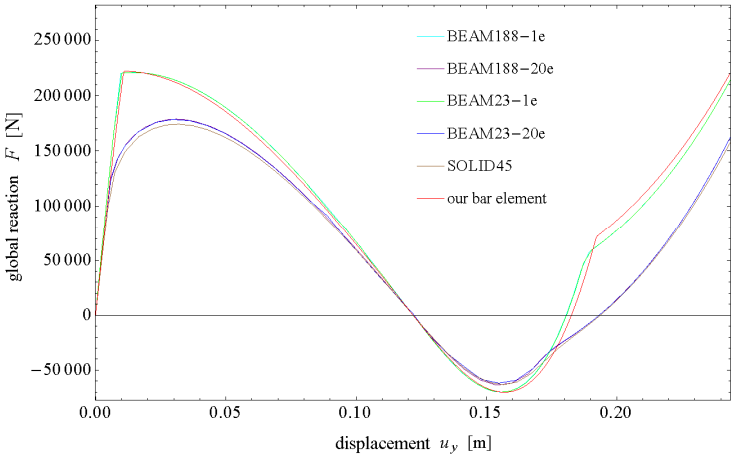

Fig. 9 *Global reaction F – common hinge displacement u_y response for the bar with kinematic hardening*

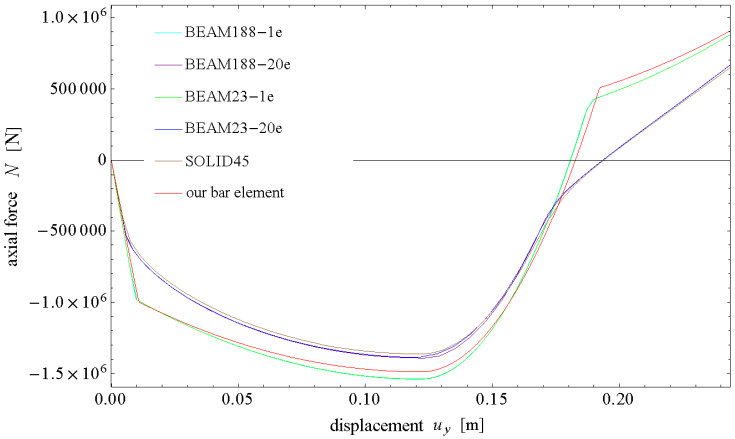

Fig. 10 *Axial force N – common hinge displacement u_y response for the bar with kinematic hardening*

Evaluation

The results of numerical experiments of the von Mises structure stress in the elasto-plastic area are presented graphically in the form of the process of axial forces N and reactions F in dependence on the vertical displacement u_y of common node.

From the dependence of axial forces N, as well as from the results presented in it can be concluded that the stiffness of our bar element is higher by approximately 2.5% than the stiffness of the spatial model consisting of SOLID45 elements. Higher stiffness than our bar element (and thus higher levels of axial force N and reaction F) is shown by models with one beam element BEAM23 or BEAM188, for which the deviation from the results obtained by spatial model is above 6%. The resulting percentage differences between the maximum values of axial forces N obtained by one-dimensional models and spatial models are summarized in *Table 3*.

PERCENT DIFFERENCE IN MAXIMUM VALUES OF AXIAL FORCES N DETERMINED BY NEW BAR ELEMENT AND BY ANSYS MODELS

Table 3

percentage difference of axial forces				
$\frac{(BEAM23/1e) - SOLID45}{SOLID45}$	$\frac{(BEAM23/100e) - SOLID45}{SOLID45}$	$\frac{(BEAM188/1e) - SOLID45}{SOLID45}$	$\frac{(BEAM188/100e) - SOLID45}{SOLID45}$	$\frac{our\ bar\ elem. - SOLID45}{SOLID45}$
6.01%	2.43%	6.19%	2.84%	2.41%

It can be concluded from the results that the courses of axial forces and reactions determined by our element are in better compliance with the solution obtained by spatial model SOLID45 than the courses obtained by

models with beam elements BEAM23, 188, especially for models with isotropic hardening material.

Significant differences in the course of forces between the models with one element and the models with fine mesh occur in the area of transition from elastic to elasto-plastic state.

This difference is caused by:

- in the case of models with one element (new bar element, beam models) is necessary to provide "mean" value of the yield stress σ_y to determine limits of transition into elasto-plastic state for the entire element, when after exceeding the stress limit, the elastic stiffness matrix [2.16] of new element turns into elasto-plastic matrix [2.20],
- in contrast to models with more elements that result in a gradual transition of the model into elasto-plastic state by plasticization of particular elements in dependence from stiffness and yield stress of the element.

This deviation also occurs in other models consisting of one beam elements (BEAM23, 188). A more significant increase of the difference in the course of axial force can be observed in case of considering the material with kinematic hardening comparing to the isotropic hardening material. With increasing axial force (i.e. an increase in the loading of a bar in elasto-plastic area) the difference between the results obtained by one new bar element and results from models decreases. In the case of considering material with isotropic hardening, the process of axial force obtained from solution by one new non-linear bar element is in good agreement with the results obtained from the multi-element models also in area of elastic

unloading of the bar and tensile stress after exceeding yield stress in the tensile area. This compliance is not significantly affected by the degree of the polynomial of the stiffness variability or by the ratio of maximum and minimum stiffness in the bar.

The difference in maximum values of axial forces determined by a new bar element and SOLID45 spatial model is less than 2.0% only in cases where the ratio of the maximum and minimum stiffness in the bar is less than 3.0.

The results of numerical experiments lead to the following conclusions:

- deviation between the value of the axial force maximum in a nonlinear bar of variable stiffness and the value obtained by a spatial model SOLID45 compared for all variations was at the level of 3.0% (or less) at a stress of the bar in flexible area,
- with increasing degree of the polynomial of variability stiffness, this difference decreases slightly,
- numerical experiments show a good agreement with the results of solving a new bar in the elasto-plastic deformation areas with spatial model in the ANSYS programme, especially when considering the material with isotropic hardening,
- significant difference in the course of axial forces or reactions determined by a new element compared to the spatial model and the model with higher density of division by BEAM elements can be reported when considering the material with kinematic hardening and stiffness ratio in the bar greater than 3.0,
- significant differences between the results obtained by the new bar element and the models with division into a larger number of elements

occur after exceeding the yield stress, and are caused by the transition of the entire bar from elastic to elasto-plastic state. This phenomenon occurs even in models with one classic BEAM element. During further increase of loading, this difference in the course of forces decreases more significantly, namely in the bars from material with isotropic hardening.

2.3 Sandwich bar element with variable stiffness

Implementation of the new advanced materials such as composites, sandwich structures or functionally graded materials into the design and production calls for designing of an appropriate model of the material. Due to a number of variables that control the design of a functionally graded microstructure, the full potential of FGM requires the development of appropriate strategies for modelling of their mechanical or thermo-mechanical properties.

Functionally graded materials (FGM) are a new generation of structural materials, in which the microstructure is purposefully spatially changed due to the uneven distribution of hardening component(s). Achieving such a state is possible by using hardening components of different properties, size and shape of the particles or by continuous gradual substitution of hardening components (fibres and matrices). This is most often achieved by creating FGM by plasma spraying or powder metallurgy. The result is a microstructure that is formed by a continuous (or discrete) change in macroscopic, electrical, thermal and mechanical properties.

FGM are suitable materials e.g. for the so-called thermal barrier in applications involving large temperature gradients, from the aircraft and rocket engines up to the use in microelectronic circuits or MEMS.

Without homogenizing the material properties of such materials, the non-linear component analysis would require creation of very fine finite element mesh, and even the time-consuming preparation of the model and the solution process itself would be significant. Macro-mechanical modelling of effective material properties of such composites is based on different homogenization procedures.

By mixing two or more components we can achieve a synergic effect when the properties of newly produced material are better than the properties of individual components. These new materials are characterized by continuous or discontinuous variation of material properties. Along with the development of these materials to improve the calculation precision and description of material properties in the numerical simulations, new methods of homogenization are being developed (27, 36, 40), or the already existing procedures are being improved (54, 55). Recently, also multi-scale methods are elaborated and are starting to be applied (26, 35).

One way of macroscopic modelling of mechanical properties of materials with heterogeneous microstructure is their homogenization and determination of effective material properties of the composite using mixing rules. The simplest mixing rule by which we can determine the average effective material properties is based on the assumption that the material properties of the composite are the sum of material properties of each component multiplied by its volume fraction. The resulting effective

property p_e of the bi-component composite consisting of the matrix with property p_m and the hardening phase p_f is determined by

$$p_e = v_f p_f + v_m p_m \qquad [2.27]$$

where v_f, v_m are the volume fractions of the matrix and the hardening phase, for which in each point of the material is valid $v_f + v_m = 1$.

In this part of the study, the extended mixing rule published in (54, 55) is used. In the first step is considered a bi-component composite material with a variable change in the modulus of elasticity and the volume ratio of both components along the longitudinal axis of a bar composite (single-direction composite). For homogenization of material properties of such composite, in section 2.3.1 is described the procedure allowing to derive the relation describing variability of the effective longitudinal elastic modulus $E_L(x)$ of the composite.

In the second part, the process of homogenization of the material properties of the sandwich element for the extended multi-layer composite is designed. For such a bar of constant double symmetric cross-section with variation of material properties of individual composite layers, the homogenization process of material properties of multilayer material is then derived. The procedure of material property homogenization is in accordance with the laminate theory (2, 54, 55). Delamination of the sandwich material is not considered. This procedure allows homogenising properties of composite and sandwich materials with spatially varying volume ratio of the components and their material properties.

With the proposed mixing rule and the procedure of homogenization, the homogenized effective properties were calculated and the stiffness matrices of non-linear bar element were assembled.

2.3.1 Single-layer composite bar element with variable stiffness

We consider a bar of constant symmetrical cross-section made of the two-component composite with symmetric distribution of both components in the cross section of the bar, to prevent the occurrence of flexural components of deformation at tensile or compressive stress of the bar.

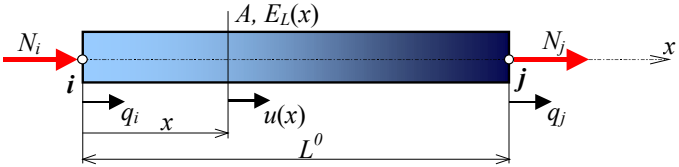

Fig. 11 *Single-layer composite bar*

In order to implement the variability of the composite bar element stiffness into our non-linear solution and derive stiffness matrices of the single-layer composite two-node bar element, it is necessary to determine the variability of the effective longitudinal modulus $E_L(x)$, that will represent a continuous variation of mechanical properties of the composite material in the direction of the axis of the bar. After determining the effective longitudinal modulus of elasticity, it is possible to derive the stiffness matrices of the composite bar element by the procedure referred to in section 2.1.

The prerequisite for the solution is the loading of element with variable stiffness only in elastic area. Also in this case, we consider polynomial variability of the modulus of fibre elasticity $E_f(x)$ and the matrix $E_m(x)$, which can be described by polynomials similar to [2.1].

In the following text, E_{fi}, E_{mi} will label the elastic modulus of fibres or matrix at the first node i of the element, and $\eta_{Ef}(x)$ or $\eta_{Em}(x)$ are the polynomials describing the variation of elastic modulus of fibre or matrix.

Such variability of elasticity modulus can be caused by temperature field generated by passing electric current (steady-state or transient), by chemical reaction, piezoelectric phenomenon, etc., acting in the element.

The volume fraction of fibres $v_f(x)$ and the matrix $v_m(x)$ as the two components of the composite material in the longitudinal axis of the bar may also be variable in accordance with [3.1] whereby in each point of the body is valid

$$v_m(x) + v_f(x) = 1 \quad . \qquad [2.28]$$

By consideration of constant mechanical properties of the fibres and matrix, the effective longitudinal modulus $E_L(x)$ can be determined by a mixing rule for two-component laminate composites known from literature (3, 13, 27). By exchange of constant values of elasticity moduli and volume fractions of the fibres and matrix conditions describing the variables change in any element point along the longitudinal axis, we obtain advanced mixing rules to determine the function describing the change in the effective longitudinal elastic modulus $E_L(x)$ in the form of polynomial (54, 55)

$$E_L(x) = v_f(x)\, E_f(x) + v_m(x)\, E_m(x) = E_{Li}\, \eta_{E_L}(x) \qquad [2.29]$$

where $E_{Li} = v_{fi}\, E_{fi} + (1 - v_{fi}) E_{mi}$ is value of effective longitudinal elastic modulus in first node *i* of the element and

$$\eta_{E_L}(x) = \frac{v_f(x)\, E_f(x) + v_m(x)\, E_m(x)}{v_{fi}\, E_{fi} + v_{mi}\, E_{mi}} \qquad [2.30]$$

is a polynomial describing the variation of the effective longitudinal elasticity modulus of whole composite.

The local non-linear stiffness matrix of bar element with the effective modulus $E_L(x)$ has the form

$$\mathbf{K} = \frac{AE_{Li}}{d'_{2E_L}}\left[1 + \frac{3}{2}(\lambda - 1)L^0 \frac{\overline{d'_{2E_L}}}{(d'_{2E_L})^2} + \frac{1}{2}(\lambda - 1)^2 (L^0)^2 \frac{\overline{\overline{d'_{2E_L}}}}{(d'_{2E_L})^3}\right]\begin{bmatrix} 1 & -1 \\ -1 & 1 \end{bmatrix} \qquad [2.31]$$

where d'_{2E_L}, $\overline{d'_{2E_L}} = \int_0^{L^0} (d''_{2E_L}(x))^2\, dx$, $\overline{\overline{d'_{2E_L}}} = \int_0^{L^0} (d''_{2E_L}(x))^3\, dx$ are transfer constants of the bar of homogenised properties for elastic area of loading based on the second derivative of the transfer function $d''_{2E_L}(x) = 1/\eta_{E_L}(x)$.

For the calculation of the transfer constants the same algorithm is used as in section 2.1.2.

We calculate axial force in the bar from modified equation [2.17], where we replace the constant transfer d'_{2e} to d'_{2E_L}.

$$N_i = -\frac{AE_{Li}}{d'_{2E_L}}\left[1+\frac{3}{2}(\lambda-1)L^0\frac{\overline{d'_{2E_L}}}{(d'_{2E_L})^2}+\frac{1}{2}(\lambda-1)^2(L^0)^2\frac{\overline{\overline{d'_{2E_L}}}}{(d'_{2E_L})^3}\right](\lambda-1)L^0 \quad [2.32]$$

Similarly, changes the local nonlinear tangent stiffness matrix [2.13] to

$$\mathbf{K}^T = \frac{AE_{Li}}{d'_{2E_L}}\left[1+3(\lambda-1)L^0\frac{\overline{d'_{2E_L}}}{(d'_{2E_L})^2}+\frac{3}{2}(\lambda-1)^2(L^0)^2\frac{\overline{\overline{d'_{2E_L}}}}{(d'_{2E_L})^3}\right]\begin{bmatrix}1 & -1\\ -1 & 1\end{bmatrix} \quad [2.33]$$

2.3.2 Effective material properties of symmetric multilayer sandwich bar

Using relationships described in the previous part of this study, the procedure for calculating the effective homogenized properties of multilayer sandwich material with a continuous change in the modulus of elasticity of the fibres and the matrix along the longitudinal axis of the element (e.g., caused by non-homogeneous thermal field in the bar) can be derived. It is necessary to make it possible to describe changes of elasticity moduli $E_m(x)$ a $E_f(x)$ of both components of the composite (matrix and reinforcing phase) by polynomial in the form [2.1] in each layer k. Analogously, it is necessary to consider the variability of the volume fractions of both components $v_m(x)$, $v_f(x)$ of the composite and also the polynomial change in coefficients of thermal expansion $\alpha_m(x)$, $\alpha_f(x)$. In general, different material properties with varying degrees of variability in each of the k-th layer may be assumed.

Volume fractions of fibres v_f and matrix v_m and materials properties of fibres E_f and matrix E_m are considered to be constant only across the width

of the element b and in the thickness direction of individual layers h^n (Fig. 12). The bar cross-sectional area of each layer is considered to be constant along the entire length of the bar. The bar element with such a defined variability of material properties will be loaded in the elastic area.

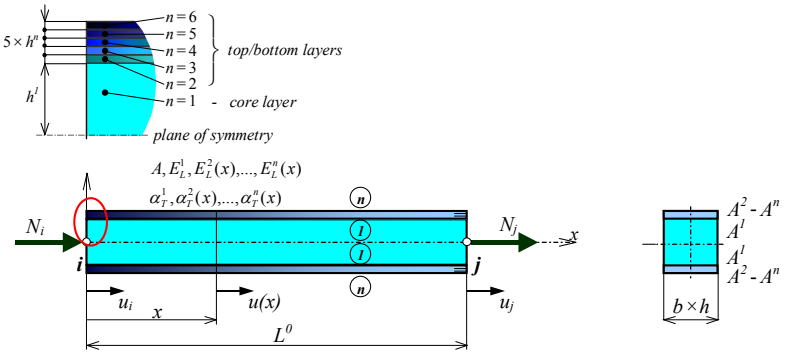

Fig. 12 *Double symmetric multilayered sandwich bar element with variation of stiffness in initial state*

2.3.2.1 Variation of material properties and volume fractions of composite constituents

In the case of multilayer composite material, we consider uniaxial polynomial change in elastic modulus of fibres $E_f^k(x)$ and matrix $E_m^k(x)$ in each of the k-th sandwich layer. Volume fractions of fibres $v_f^k(x)$ and matrix $v_m^k(x)$ as the composite components are described by similar polynomial expressions.

The effective longitudinal elasticity modulus of *k*-th layer changes according to modified equation [2.29] for single-layer composite rewritten to

$$E_L^k(x) = v_f^k(x)\,E_f^k(x) + v_m^k(x)\,E_m^k(x) = E_{Li}^k\,\eta_{E_L}^k(x) \qquad [2.34]$$

where $E_{Li}^k = v_{fi}^k\,E_{fi}^k + v_{mi}^k\,E_{mi}^k = v_{fi}^k\,E_{fi}^k + (1 - v_{fi}^k)E_{mi}^k$ is the value of effective longitudinal modulus in first node *i* of the bar and *k*-th layer

$$\eta_{E_L}^k(x) = 1 + \frac{\eta_{v_f}^k(x)\,\eta_{E_f}^k(x) + \eta_{v_m}^k(x)\,\eta_{E_m}^k(x)}{E_{Li}^k} = 1 + \sum_{q=1}^{s+t} \eta_{E_L q}^k\,x^q \qquad [2.35]$$

is the relation for effective longitudinal elasticity modulus variation of the *k*-th layer. Order of the polynomial [2.35] depends on the constituent material properties and the volume fractions variation. Index $k \in \langle 1; n{=}6 \rangle$ denotes the layer number in the upper/lower symmetrical part of the bar (see Fig. 12).

2.3.2.2 Variation of thermal expansion coefficient one layer in sandwich bar

We consider variation of fibres thermal expansion coefficient $\alpha_{Tf}^k(x)$ and matrix thermal expansion coefficient $\alpha_{Tm}^k(x)$ in *k*-th layer of sandwich bar described by polynomials in form [2.1].

The effective longitudinal thermal expansion coefficient $\alpha_{TL}^k(x)$ of *k*-th layer can be calculated using extended Schapery approximation (60)

$$\alpha_{TL}^{k}(x)=\frac{v_f^k(x)\alpha_{Tf}^k(x)E_f^k(x)+v_m^k(x)\alpha_{Tm}^k(x)E_m^k(x)}{v_f^k(x)E_f^k(x)+v_m^k(x)E_m^k(x)} \qquad [2.36]$$

Expression [2.36] is not polynomial and expansion to Taylor´s series is necessary to be used to convert it into polynomial form.

2.3.2.3 Variation of homogenized material properties of sandwich element

Let us define a cross-sectional area ratio of *k*-th layer

$$r_A^k = 2A^k / A \qquad [2.37]$$

where A^k is cross-sectional area of *k*-th layer and A is total cross-sectional area of the bar. Then, the homogenized effective longitudinal elasticity modulus of the whole element $E_L^H(x)$ in the polynomial form is given by

$$E_L^H(x)=\sum_{k=1}^{n} r_A^k\, E_L^k(x)=E_{Li}^H\,\eta_{E_L^H}(x) \qquad [2.38]$$

where E_{Li}^H is the value of homogenized effective longitudinal elasticity modulus at node *i* and $\eta_{E_L^H}(x)$ is the polynomial of its longitudinal variation. Elasticity modulus of *k*-th layer $E_L^k(x)$ is given by equation [2.34].

The homogenized effective longitudinal thermal expansion coefficient of the whole element can be calculated from expression

$$\alpha_{TL}^{H}(x)=\frac{\sum_{k=1}^{n}\alpha_{TL}^{k}(x)E_{L}^{k}(x)}{\sum_{k=1}^{n}E_{L}^{k}(x)}=\frac{1}{E_{L}^{H}(x)}\sum_{k=1}^{n}r_{A}^{k}\,\alpha_{TL}^{k}(x)E_{L}^{k}(x) \qquad [2.39]$$

where thermal expansion coefficient of *k*-th layer $\alpha_{TL}^{k}(x)$ can be calculated using [2.36]. Equation [2.39] is necessary to convert into polynomial form using expansion to Taylor´s series.

$$\alpha_{TL}^{H}(x)=\alpha_{TLi}^{H}\,\eta_{\alpha_{TL}^{H}}(x) \qquad [2.40]$$

where α_{TLi}^{H} is the value of homogenized effective longitudinal thermal expansion coefficient at node *i* and $\eta_{\alpha_{TL}^{H}}(x)$ is the polynomial of its longitudinal variation.

2.3.2.4 Homogenized stiffness matrices of the sandwich bar element

The procedure of the stiffness matrices of homogenized sandwich bar derivation is identical to the procedure in section 2.1. In the differential equation [2.3] the constant cross-section is considered, and the variability of modulus of elasticity is determined by the relationship [2.38]. Thus the relation [2.3] determining the relative deformation of in the bar is changed to

$$\frac{du(x)}{dx}=\frac{N(x)}{AE_{L}^{H}(x)}=\frac{N(x)}{AE_{Li}^{H}\,\eta_{E_{L}^{H}}(x)} \qquad [2.41]$$

The second derivative of the transfer function $d''_{2E_L^H}(x) = 1/\eta_{E_L^H}(x)$ is defined by polynomial of variability $\eta_{E_L^H}(x)$ of the homogenized effective longitudinal modulus of elasticity in equation [2.38]. After modifying the shape functions of bar element, the displacement of an arbitrary point of the bar can be expressed by the relationship

$$u(x) = \left(1 - \frac{d'_{2E_L^H}(x)}{d'_{2E_L^H}}\right) u_i + \frac{d'_{2E_L^H}(x)}{d'_{2E_L^H}} u_j = \phi_{1i}\, q_i + \phi_{1j}\, q_j \qquad [2.42]$$

After implementation of shape functions [2.42] into equations [2.8], [2.9], [2.10] and [2.11] local stiffness matrix of the bar **K** change to

$$\mathbf{K} = \frac{AE_{Li}^H}{d'_{2E_L^H}} \left[1 + \frac{3}{2}(\lambda - 1) L^0 \frac{\overline{d'_{2E_L^H}}}{(d'_{2E_L^H})^2} + \frac{1}{2}(\lambda - 1)^2 (L^0)^2 \frac{\overline{\overline{d'_{2E_L^H}}}}{(d'_{2E_L^H})^3}\right] \begin{bmatrix} 1 & -1 \\ -1 & 1 \end{bmatrix} \qquad [2.43]$$

where $\overline{d'_{2E_L^H}} = \int_0^{L^0} (d''_{2E_L^H}(x))^2 dx$, $\overline{\overline{d'_{2E_L^H}}} = \int_0^{L^0} (d''_{2E_L^H}(x))^3 dx$ are transfer constants derived from a polynomial describing variability of homogenized effective longitudinal modulus of elasticity.

The relationship [2.17] for calculation of axial force in the element will be changed into

$$N_i = -\frac{AE_{Li}^H}{d'_{2E_L^H}} \left[1 + \frac{3}{2}(\lambda - 1) L^0 \frac{\overline{d'_{2E_L^H}}}{(d'_{2E_L^H})^2} + \frac{1}{2}(\lambda - 1)^2 (L^0)^2 \frac{\overline{\overline{d'_{2E_L^H}}}}{(d'_{2E_L^H})^3}\right] (\lambda - 1) L^0 \qquad [2.44]$$

Relationship [2.15] for determining the tangential stiffness matrix of the homogenized material of the sandwich bar will be changed in the form

$$\mathbf{K}^{T}=\frac{AE_{Li}^{H}}{d'_{2E_L^H}}\left[1+3(\lambda-1)L^0\frac{\overline{d'_{2E_L^H}}}{(d'_{2E_L^H})^2}+\frac{3}{2}(\lambda-1)^2(L^0)^2\frac{\overline{\overline{d'_{2E_L^H}}}}{(d'_{2E_L^H})^3}\right]\begin{bmatrix}1 & -1\\ -1 & 1\end{bmatrix} \quad [2.45]$$

2.4 Inclusion of the thermal field action in a sandwich bar

In this paper, the relations for the implementation of the thermal field effect in the bar to its deformation are derived. Let us assume that the bar operates in the stationary temperature field, whereby the temperature is changed along the longitudinal axis of the bar. At the same time, we consider the longitudinal variation of the coefficient of thermal expansion of each layer $\alpha_{TL}^{k}(x)$, which can be described by polynomial [2.36]. The effect of thus operating the thermal field is reflected through the contribution of forces induced by thermal field into the vector of nodal forces on the right-hand side of equation [1.7]. The task is solved as a weak coupled problem.

In the linear FEM theory, the equivalent nodal thermal load is defined by the relationship

$$\mathbf{F}_{\varepsilon_0}=\begin{bmatrix}F_i^{th}\\ F_j^{th}\end{bmatrix}=\int_{V^0}\mathbf{B}_L^{\mathrm{T}}\mathbf{D}\boldsymbol{\varepsilon}_{\mathbf{0}}\,dV\begin{bmatrix}-1\\ 1\end{bmatrix} \quad [2.46]$$

For the bar element, we can overwrite the previous relationship to

$$\begin{bmatrix}F_i^{th}\\ F_j^{th}\end{bmatrix}=\int_{L^0}\mathbf{B}_L^{\mathrm{T}}E\,\alpha_T\,\Delta T\,A\,dx\begin{bmatrix}-1\\ 1\end{bmatrix} \quad [2.47]$$

Using shape functions ϕ_{lk} for elastic loading area, the strain transformation matrix can be expressed by derivatives of shape functions [2.42]

$$\mathbf{B}_L = \left[\phi_{11,1}(x) \quad \phi_{12,1}(x)\right]^{\mathrm{T}} = \begin{bmatrix} -\dfrac{d''_{2E_L^H}(x)}{d'_{2E_L^H}} & \dfrac{d''_{2E_L^H}(x)}{d'_{2E_L^H}} \end{bmatrix}^{\mathrm{T}} \qquad [2.48]$$

The matrix of elastic material constants for the bar is defined by $\mathbf{D} = \left[E_L^H(x)\right]$ and the strain thermal vector is equal to $\boldsymbol{\varepsilon_0} = \varepsilon_0(x) = \alpha_{TL}^H(x)(T(x) - T_{ref})$ where T_{ref} s the reference temperature. After substituting these relations into [2.46] this relationship can be modified in the form (56, 57)

$$\begin{bmatrix} F_i^{th} \\ F_j^{th} \end{bmatrix} = \int_0^{L^0} \frac{d''_{2E_L^H}(x)}{d'_{2E_L^H}} E_L^H(x)\,\alpha_{TL}^H(x)(T(x) - T_{ref})\,A\,dx \begin{bmatrix} -1 \\ 1 \end{bmatrix} \qquad [2.49]$$

For the bar with the longitudinal variability of the homogenized modulus of elasticity $E_L^H(x)$ according to [2.38] the homogenized effective longitudinal coefficient of thermal expansion $\alpha_{TL}^H(x)$ determined by [2.40] and loaded by thermal field represented by the change in temperature $T(x) = T_i\,\eta_T(x)$ v along the longitudinal axis of the bar element. Effective thermal nodal forces can be determined from the modified relation [2.49]

$$\begin{bmatrix} F_i^{th} \\ F_j^{th} \end{bmatrix} = \begin{bmatrix} -1 \\ 1 \end{bmatrix} \frac{E_{Li}^H\,A\,\alpha_{TLi}^H\,\Delta T_i}{d'_{2E_L^H}} \int_0^{L^0} \eta_{\alpha\Delta T}(x)\,dx \qquad [2.50]$$

where $\Delta T_i = T_i - T_{ref}$ represents the temperature difference between the temperature T_i in the node i of the element by chosen reference temperature T_{ref}. The polynomial $\eta_{\alpha\Delta T}(x)$ is represented by

$$\eta_{\alpha\Delta T}(x) = \eta_{\alpha_{TL}^{H}}(x)\,\eta_{\Delta T}(x) \qquad [2.51]$$

where $\eta_{\Delta T}(x) = (T(x) - T_{ref})/(T_i - T_{ref})$ is the polynomial describing the variability of the thermal field, and the polynomial $\eta_{\alpha_{TL}^{H}}(x)$ describing the longitudinal variability of the homogenized thermal expansion coefficient can be expressed by the equation [2.40]. Relative deformation of the temperature $\varepsilon_0(x)$ at any point of the element made of the material of homogenized properties can be calculated from equation

$$\varepsilon_0(x) = \alpha_{TL}^{H}(x)\,(T(x) - T_{ref}) = \alpha_{TLi}^{H}\,\Delta T_i\,\eta_{\alpha\Delta T}(x) \qquad [2.52]$$

Deformation Δu_T of the bar caused by thermal loading not dependent on the stiffness of the bar and is equal

$$\Delta u_T = \int_0^{L^0} \varepsilon_0(x)\,dx = \alpha_{TLi}^{H}\,\Delta T_i \int_0^{L^0} \eta_{\alpha\Delta T}(x)\,dx \qquad [2.53]$$

For inclusion of thermal forces, it is sufficient to change the right side of [1.7] to

$$\mathbf{F} = \begin{bmatrix} N_i \\ N_j \end{bmatrix} + \begin{bmatrix} F_i^{th} \\ F_j^{th} \end{bmatrix} \qquad [2.54]$$

2.5 Normal stress in sandwich bar

2.5.1 Normal stress caused by structural axial loading

The expression for calculation of the effective longitudinal strain caused by structural loading in elastic area, we get from the derivation of equations [2.42] and [2.52] in the form (60)

$$\varepsilon_{struc}(x) = \frac{du(x)}{dx} - \varepsilon_0(x) = \frac{(q_j - q_i) - \Delta u_T}{\eta_{E_L^H}(x)\, d'_{2E_L^H}} \quad . \qquad [2.55]$$

The effective normal stress in the homogenized bar is then

$$\sigma_L^H(x) = \varepsilon_{struc}(x)\, E_L^H(x) \quad . \qquad [2.56]$$

Real stress in the *k*-th layer is

$$\sigma^k(x) = \varepsilon_{struc}(x)\, E_L^k(x) \quad . \qquad [2.57]$$

2.5.2 Normal stress caused by temperature loading

The thermal stresses in the bar are caused by difference between thermal expansion coefficient $\alpha_{TL}^k(x)$ of individual layers and homogenized effective thermal expansion coefficient $\alpha_{TL}^H(x)$ of whole element. Thermal stress in *k*-th layer can be calculated from

$$\sigma_{th}^k(x) = \left(\alpha_{TL}^H(x) - \alpha_{TL}^k(x)\right)\left(T(x) - T_{ref}\right)E_L^k(x) \qquad [2.58]$$

2.5.3 Total strain and stress

Total normal stress in *k*-th layer is equal to the sum of structural [2.57] and thermal stress [2.58]

$$\sigma_{total}^{k}(x) = \sigma^{k}(x) + \sigma_{th}^{k}(x) \qquad [2.59]$$

The total displacement of an arbitrary point of the bar under elastic loading is determined by the sum of the displacement caused by structural and thermal loading and is expressed by equation (59, 60)

$$u(x) = \left(1 - \frac{d'_{2e}(x)}{d'_{2e}}\right) q_i + \frac{d'_{2e}(x)}{d'_{2e}} q_j - \frac{d'_{2e}(x)}{d'_{2e}} u_T(L^0) + u_T(x) \qquad [2.60]$$

2.6 Numerical experiments for evaluation of the properties of the sandwich bar element with variable stiffness

2.6.1 Models used in problems of the sandwich bar stress

To assess whether the stiffness matrices of the new geometrically nonlinear bar element with the effective modulus of elasticity of the homogenized bar, derived in section 2.4, allow to accurately measure the stiffness variability of the real composite or sandwich bar, the finite element programs to solve selected problems were developed in the MATHEMATICA software environment. The compiled programmes allowed solving geometrically nonlinear problems in the elastic stress area of the new bar element from the material of homogenized properties. The possibility of taking into account the

temperature field effect in the bar, as derived in section 2.4, was implemented into the programmes. The programmes were extended also to the calculation of stresses in the layers of sandwich bar according to the relationships described in section 2.5.3. In solving of all the problems, only one bar element was used, i.e. the problem was always modelled by the procedure *one line = one element*. The full square, along the length constant cross-section was considered.

As the reference solutions for obtaining comparative results to assess the properties of the new element the following simulation models were created in the ANSYS:

- Model BEAM3 – one-dimensional model consisting of 20 beam elements BEAM3,
- Model BEAM188 – one-dimensional model consisting of 20 beam elements BEAM188,
- spatial model consisting of the mesh of 37200 elements SOLID45 that allowed faithfully enough to describe the variability of cross section and material properties and determine the course of stresses in individual layers of the sandwich element,
- PLANE42 – the two-dimensional model with an identical mesh topology, used in repeated analyzes to determine the course of stresses to reduce computational time.

2.6.2 Numerical experiment

To assess the structural behaviour of sandwich bar element of homogenized properties, there was considered the two-node 12-layer sandwich bar with constant cross-section in **Fig. 12** placed in the structure according to **Fig. 6**a. Layers and their geometric shape of the considered bar are symmetrical in relation to the neutral plane. The material of layers consists of two components: the *matrix* material NiFe labeled by *m* infex and the *fibre* material Tungsten labelled by *f* index.

Geometric parameters (**Fig. 12**) of the bar and material properties are arranged in Table 4. The constant linear elastic material properties of the matrix and the fibres (E_m = konst. and E_f = konst.) were considered in the numerical experiment. The material of the sandwich structure intermediate layer (core, labelled by number 1) was considered with the properties of pure matrix with modulus of elasticity E_m. Symmetrical pairs of layers labelled $k = \langle 2,...,6 \rangle$ were created by asymmetric mixing of both components of the matrix and the fibres, wherein the ratio of the components in individual layers was different.

The considered values of the parameters in this equation for the relevant k^{th} layer are specified in Table 5. The volume fibre ratios were considered constant in width-wise direction b and height-wise direction h^k každej vrstvy. There is assumed only a linear change of the volume fibre ratios in the direction of the length L^0 of each layer, i.e. the mechanical properties of the whole sample are changing in the direction of its height and length. In the initial node i, the volume fraction of fibres (matrix) was considered

different in each layer and in the terminal node j of the element, it was considered constant in all layers.

MATERIAL PROPERTIES OF CONSTITUENTS AND GEOMETRICAL PARAMETERS Table 4

material properties		
Tungsten (*fibres*)	elasticity modulus of fibres	$E_f = 400$ GPa
	thermal expansion coefficient of fibres	$\alpha_{Tf} = 5.3\times10^{-6}$ K^{-1}
NiFe (*matrix*)	elasticity modulus of matrix	$E_m = 255$ GPa
	thermal expansion coefficient of matrix	$\alpha_{Tm} = 1.5\times10^{-5}$ K^{-1}

geometrical parameters of specimen	
specimen length	$L^0 = 0.1$ m
specimen width	$b = 0.01$ m
specimen height	$h = 0.01$ m
total number of layers (incl. core)	$2n = 12$ (2×6)
initial angle	$\alpha^0 = 7°$
cross-sectional area	$A = 0.0001$ m^2
cross-sectional area of 1st layer	$A^1 = 0.00004$ m^2
cross-sectional area of kth layer	$A^k = 0.000002$ m^2
total thickness of face layers	$t = 0.001$ m
thickness of 1st layer	$h^1 = 0.004$ m
thickness of kth layer	$h^k = 0.0002$ m

PARAMETERS OF OLYNOMIAL VARIATION OF FIBRE VOLUME FRACTION ALONG THE X-AXIS OF THE BAR Table 5

k-th layer	1	2	3	4	5	6
v_{fi}^k	0	0.6	0.7	0.8	0.9	1.0
η_{vf1}^k	0	– 30/6	– 40/7	– 50/8	– 60/9	– 70/10

Volume fraction of the composite components changes linearly along each *k*-th layer in accordance with the relation [3.28]

$$\nu_f^k(x) = 1 - \nu_m^k(x) = \nu_{fi}^k(1 + \eta_{vf1}^k\, x) \qquad k \in \langle 1,...,6 \rangle \qquad \text{[P1]}$$

List of ν_{fi}^k, η_{vf1}^k parameters is given in Table 5.

By substituting coefficients ν_{fi}^k, η_{vf1}^k listed in Table 5 into relation [P1] we obtain polynomials describing the variation of volume fractions of the composite hardening component $\nu_f^k(x)$ in individual composite layers. Then using the equation [2.34] polynomials of effective longitudinal modulus of elasticity $E_L^k(x)$ of the *k*-th composite layer of the sandwich was determined. Thus designed polynomials describing the variation of the effective modulus of elasticity in each layer are shown in the following table.

VARIATION OF ELASTICITY MODULUS ALONG THE LONGITUDINAL X-AXIS OF THE BAR IN K-TH LAYER Table 6

k-th layer	*variation of elasticity modulus of k-th sandwich layer* $E_L^k(x)$ [GPa]
1	255
2	342 (1 – 1.271929824 *x*)
3	356.5 (1 – 1.626928471 *x*)
4	371 (1 – 1.954177898 *x*)
5	385.5 (1 – 2.256809338 *x*)
6	400 (1 – 2.5375 *x*)

The effective homogenized elasticity modulus $E_L^H(x)$ of whole sandwich is calculated by expression [2.38] using the effective elasticity moduli $E_L^k(x)$ (Table 6) of sandwich layers

$$E_L^H(x) = 278{,}2\,(1 - 0{,}5212077642\,x) \quad \text{[GPa]} \qquad \text{[P2]}$$

while for the coefficient of the ratio of cross sectional areas [2.37] on the basis of geometric dimensions in *Table 4* is valid: $r_A{}^1 = 0{,}8$ a $r_A{}^k = 0{,}04$ for $k \in \langle 2,...,6 \rangle$. All effective elasticity moduli are shown in **Fig. 13**.

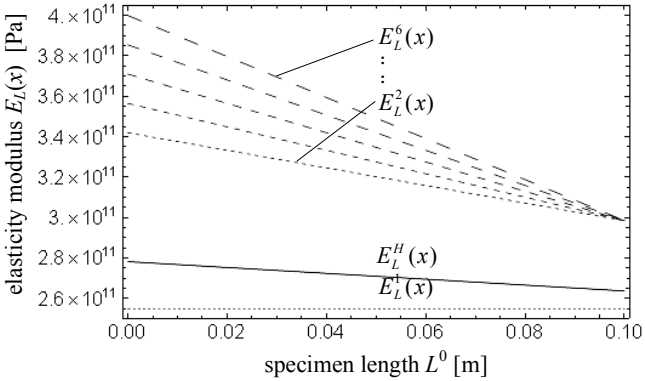

Fig. 13 *Variations of all effective longitudinal elasticity moduli*

2.6.2.1 Stress of the sandwich bar element in elastic area considering the temperature field

In this part of the numerical experiment, we considered loading of the bar structure in Fig. 5 by displacement u_y of the common node and by the stationary temperature field varying along the length of the bar, described by the relationship [P4]. Similarly, as for the elastic modulus based on the relationships derived in section 2.3.2.2, it is necessary to determine the effective coefficient of thermal expansion of individual layers $\alpha_{TL}^{k}(x)$.

VARIATION OF THERMAL EXPANSION COEFFICIENTS IN THE DIRECTION OF LONGITUDINAL ELEMENT AXIS IN EACH LAYER

Table 7

k-th layer	*variation of thermal expansion coefficient of k-th layer* $\alpha_{TL}^{k}(x)$ [K^{-1}]
1	$\alpha_{TL}^{1}(x) = 1{,}5.10^{-5}$
2	$\alpha_{TL}^{2}(x) = \frac{1{,}5686.10^{-5}}{0{,}78620 - x} - 1{,}1758.10^{-5}$
3	$\alpha_{TL}^{3}(x) = \frac{1{,}1764.10^{-5}}{0{,}61465 - x} - 1{,}1758.10^{-5}$
4	$\alpha_{TL}^{4}(x) = \frac{9{,}4116.10^{-6}}{0{,}51172 - x} - 1{,}1758.10^{-5}$
5	$\alpha_{TL}^{5}(x) = \frac{7{,}8430.10^{-6}}{0{,}44310 - x} - 1{,}1758.10^{-5}$
6	$\alpha_{TL}^{6}(x) = \frac{6{,}7226.10^{-6}}{0{,}39408 - x} - 1{,}1758.10^{-5}$

To determine the effective coefficient of thermal expansion of *k*-th composite layer, the relationship [2.36] was used. Obtained variabilities of effective coefficients of thermal expansion of the layers thermal expansion are shown in Table 7.

Consequently, from the relation [2.39], as described in section 2.3.2.3, was determined an effective longitudinal coefficient of thermal expansion of the homogenized sandwich element $\alpha_{TL}^{H}(x)$, using the already determined coefficients of thermal expansion of individual layers $\alpha_{TL}^{k}(x)$. The resulting relationship was necessary to be transformed into the polynomial form (by the development into Taylor series) and for selected variability coefficients of thermal expansion of individual layers *k* (Table 7), the expression for the an effective homogenized longitudinal coefficient of thermal expansion has the form

$$\alpha_{TL}^{H}(x) = 1{,}2768.10^{-5} + 1{,}2783.10^{-5}\,x + 6{,}6629.10^{-6}\,x^2 + 3{,}472.10^{-6}\,x^3 + 1{,}81.10^{-6}\,x^4 + 9{,}4341.10^{-7}\,x^5 + 4{,}9171.10^{-7}\,x^6\ [\mathrm{K}^{-1}] \qquad [P3]$$

All thermal expansion coefficients are shown in **Fig. 14**.

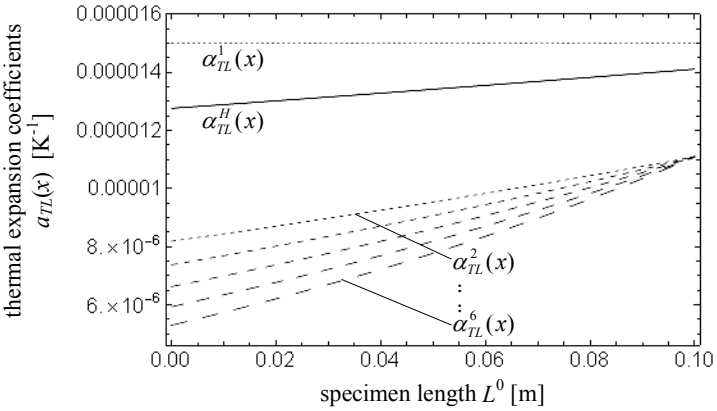

Fig. 14 *Variations of all effective thermal expansion coefficients*

Variability of the effective longitudinal coefficient of thermal expansion $\alpha_{TL}^{k}(x)$ in single layers $k \in \langle 1,...,6 \rangle$ and the whole homogenized effective longitudinal coefficient of thermal expansion $\alpha_{TL}^{H}(x)$ is described by the relationship [P3].

Variability of the effective coefficient of thermal expansion $\alpha_{TL}^{k}(x)$ (Table 7) and effective modulus of $E_{L}^{k}(x)$ Table 6 for each *k*-th layer were used to define material properties of the elements of spatial model designed in ANSYS programme. Homogenized effective material properties $\alpha_{TL}^{H}(x)$ [P3] a $E_{L}^{H}(x)$ [P2] of the whole sandwich element were used in models made by one-dimensional elements (our beam element and models with beam elements BEAM3 a BEAM188).

In all models, the steady-state effect of thermal field and temperature distribution along the length of bar was considered as a thermal load and is described by the relationship

$$T(x) = 30(1 - 2x + 4x^2) \ [^{\circ}\mathrm{C}] \ . \qquad [P4]$$

The reference temperature was $T_{ref} = 0^{\circ}\mathrm{C}$.

Statically determinate sandwich bar loaded by longitudinally varying temperature field

The first step of the numerical experiment considering the effect of the temperature field was determination of total deformation (extension) of a static 12-layer sandwich bar under the effect of temperature field described by the relationship [P4]. The resulting extensions of bar caused by temperatures for the selected simulation models are presented in the table below.

EXTENSION OF A STATICALLY DETERMINATE SANDWICH BAR LOADED BY THERMAL FIELD Table 8

	BEAM188-20e	PLANE42	SOLID45	our bar elem.
Δl [m]	0.000036753	0.000036876	0.000036895	0.000036745

Fig. 15 shows distribution of normal stresses in layers of statically determinate sandwich bar loaded only by temperature field defined by [P4]. Stress results were obtained by only one bar element and using spatial model SOLID45 with very fine mesh.

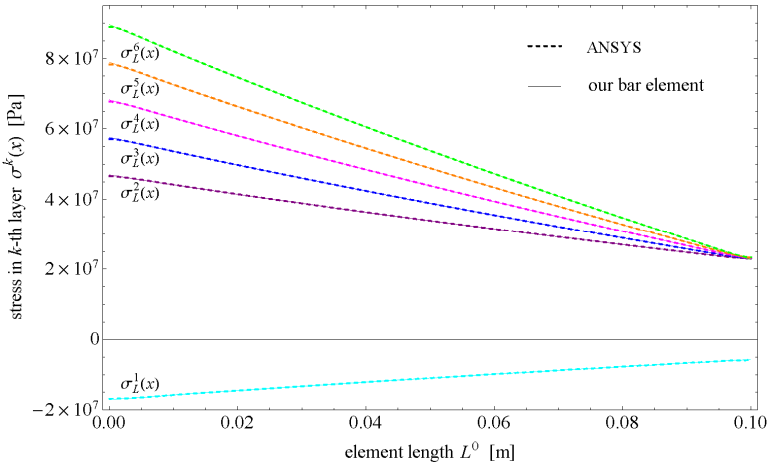

Fig. 15 *Distribution of normal stresses in individual layers of statically determinate sandwich element with consideration of thermal loading*

Statically indeterminate sandwich bar loaded by the longitudinally varying thermal field

In the second step of numerical experiment, a 12-layer sandwich statically indeterminate bar was exposed to steady thermal field with the variation of temperature defined by the relationship [P4]. The course of displacement of nodal points on the axis of the bar, obtained using the new bar element and a spatial model with elements of SOLID45 is compared Fig. 16. Calculated absolute values of reaction in bonds of statically indeterminate bar are shown in Table 9, Fig. 17a) illustrate the courses of stresses in layers statically indeterminate sandwich bar loaded only thermal field described by the relationship [P4].

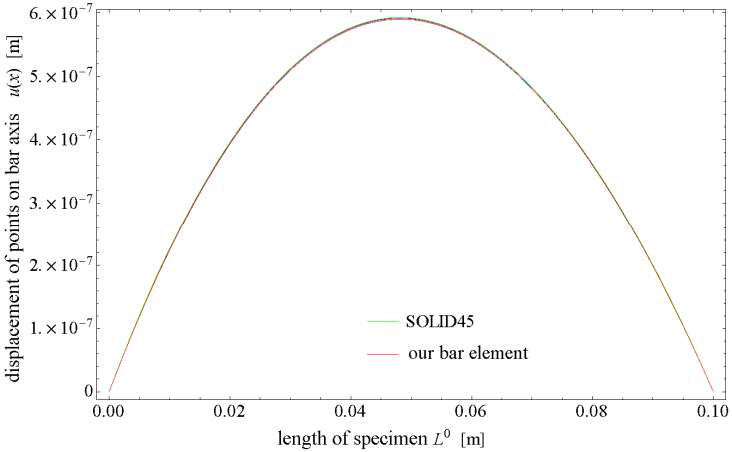

Fig. 16 *Distribution of axial displacements u_x in statically indeterminate bar with consideration of thermal loading*

REACTIONS IN CONSTRAINTS OF STATICALLY INDETERMINATE SANDWICH BAR LOADED BY TEMPERATURE FIELD Table 9

	BEAM188-20e	PLANE42	SOLID45	our bar elem.
$\|\|R\|\|$ [N]	9953.9	9964.0	9964.1	9953.69

Effective normal stress in statically indeterminate bar with homogenized material properties hold σ_L^H = –99,5369 MPa.

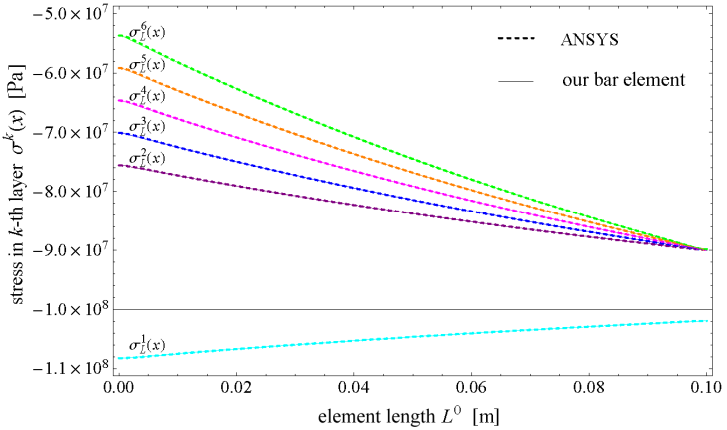

Fig. 17 *Distribution of normal stresses in individual layers of statically indeterminate sandwich element with consideration of thermal loading*

Von Mises structure with sandwich bars loaded along the longitudinally varying thermal field

In the third loading step, Von Mises structure, according to Fig. 5, was loaded by displacement u_y within the range $\langle +L^0 \sin\alpha^0 ; -L^0 \sin\alpha^0 \rangle$ so that to obtain dependence of axial force N or reaction F on the displacement u_y during deformation of the structure. Bars were also subjected to the action of steady thermal field with the variation of temperature defined by the relationship [P4]. From Fig. 18 (dependence of reaction F) a Fig. 19 (dependence of axial force N from the displacement u_y) it can be concluded that the results of the course of forces obtained with one sandwich bar element of homogenized material properties are in good agreement with the results obtained from the spatial model SOLID45. Compared with the

solution without considering the thermal loading, there was an increase of the difference between both solutions by around 0.2%. The maximum values of forces (axial N and reaction F) reached when the differences between particular results are the largest are listed in Table 10.

VALUES OF MAXIMUM FORCES OBTAINED BY OUR BAR ELEMENT AND REFERENCE ANSYS SOLUTIONS WITH CONSIDERATION OF THERMAL LOADING Table 10

axial force N [N]			
BEAM3 20 elements	BEAM188 20 elements	one new bar element	SOLID45
–113 034	–113 231	–112 446	–112 916
			
global reaction $\|\|F\|\|$ [N]			
BEAM3 20 elements	BEAM188 20 elements	one new bar element	SOLID45
3 978.78	3 982.77	3 965.42	3 975.88

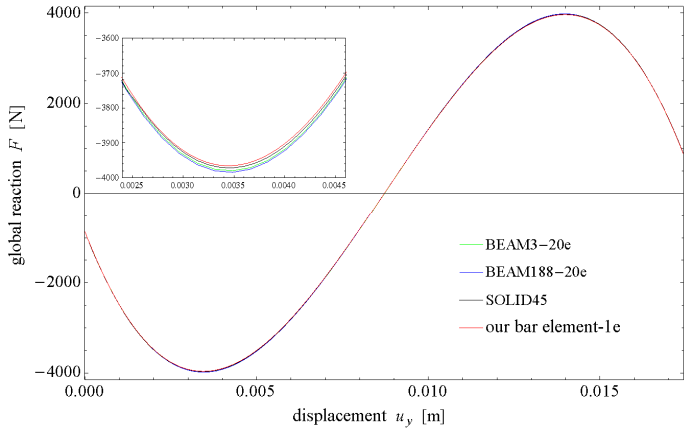

Fig. 18 *Global reaction F vs. common node displacement u_y response in the elastic bar under structural and thermal loading*

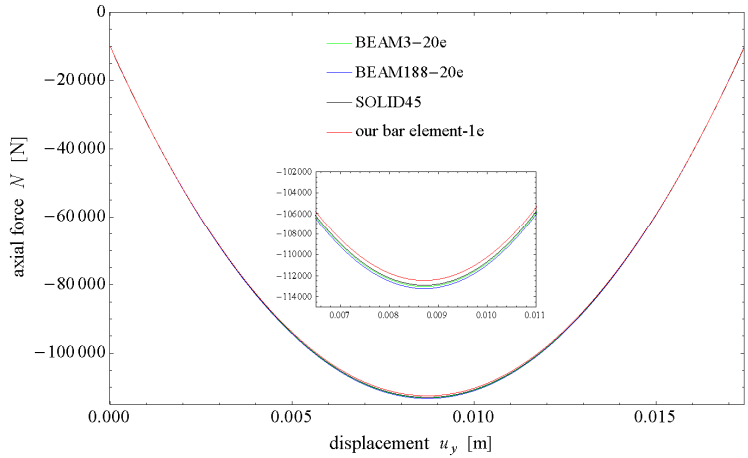

Fig. 19 *Axial force N vs. common node displacement u_y response in the elastic bar under structural and thermal loading*

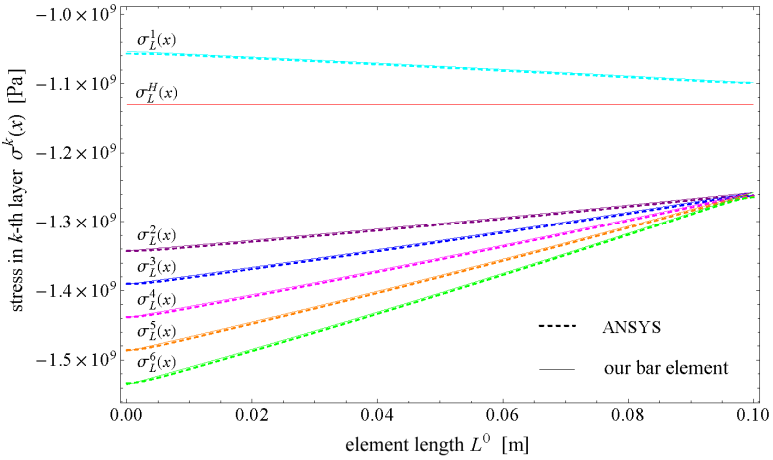

Fig. 20 *Normal stresses in layers of sandwich bar in configuration $\alpha^l = 0°$ and with consideration of thermal field*

Fig. 20 shows the courses of the total normal stresses (structural and thermal) in the line passing through the mid-height of each layer, determined from the analysis by the ANSYS using a spatial model SOLID45 and the results obtained by using one new bar element.

PERCENTAGE DIFFERENCES OF MAXIMUM FORCES OBTAINED BY OUR BAR ELEMENT AND REFERENCE ANSYS SOLUTIONS WITH CONSIDERATION OF THERMAL LOADING Table 11

axial force N			*global reaction F*		
$\frac{our\ bar - BEAM3}{BEAM3}$	$\frac{our\ bar - BEAM188}{BEAM188}$	$\frac{our\ bar - SOLID}{SOLID}$	$\frac{our\ bar - BEAM3}{BEAM3}$	$\frac{our\ bar - BEAM188}{BEAM188}$	$\frac{our\ bar - SOLID}{SOLID}$
0.523%	0.698%	0.418%	0.337%	0.437%	0.264%

Reciprocal percentage differences of the forces maxima obtained by particular models are listed in Table 11.

NORMAL STRESS IN MIDDLE OF K-TH LAYER IN LOAD STEP $\alpha^T = 0°$, WITH CONSIDERATION OF THERMAL FIELD Table 12

node	*k*-th layer:	*normal stress in k-th layer* $\sigma^k_{i(j)}$ [MPa]					
		1	2	3	4	5	6
i	our element	–1 053.15	–1 342.63	–1 390.86	–1 439.12	–1 487.36	–1 535.61
	SOLID45	–1 056.71	–1 342.78	–1 390.34	–1 437.94	–1 485.62	–1 533.45
j	our element	–1 098.72	–1 256.82	–1 256.82	–1 256.82	–1 256.82	–1 256.82
	SOLID45	–1 098.64	–1 261.63	–1 262.44	–1 263.17	–1 263.74	–1 264.11

Table 12 contains the values of normal stresses in the middle of each layer in the start and end point of element (in nodes in outer surfaces of the model). These results are obtained from the solution with one of our bar elements and from a spatial model SOLID45, and they correspond to the loading state when axial force in the bar reaches the maximum value, i.e.

the local *x*-axis of the bar is identified with the global *x*-axis. Effective normal stress in the bar of homogenized material properties reached the value $\sigma_L^H = -1\ 130.34$ MPa.

Evaluation

In this case, the properties and the accuracy of extended mixing rule described in section 2.3.2 with the application on 12-layer sandwich bar were studied. For the selected material properties of the components of composite forming individual layers of the sandwich listed in *Table 4*, based on the procedure described in section 2.3.2.3, were determined the effective moduli of the individual layers $E_L^k(x)$ and the supplementary effective homogenized modulus of elasticity $E_L^H(x)$ of the complete sandwich bar expressed by relationship [P2]. In the same way, the coefficient of thermal expansion of individual layer $\alpha_{TL}^k(x)$ (Table 7) and homogenized effective coefficient of thermal expansion $\alpha_{TL}^H(x)$ expressed by relationship [P3] were determined. Homogenized effective properties were used in one-dimensional models with a new bar element and in one-dimensional BEAM models consisting of beam elements. As a comparative solution, spatial model SOLID45 was also used, in which the variation of thermo-mechanical properties separately in each layer of spatial model was defined. To assess the accuracy of the homogenization of material properties, the problem of Von Mises structure snap-through was used. Three types of numerical experiments were performed, in which, besides structural loading, the influence of thermal

field described by the relationship [P4] was also considered. The inclusion of thermal field exposure to loading of the bar is described in section 2.4.

The results obtained using different models were prepared in the form of a table of maximum values of axial forces N and reactions F, and graphical dependencies on the displacement u_y forces during the whole deformation process. In section 2.5 were derived relationships allowing in the case of the solution of problem with one-dimensional model of homogenized material properties to determine the course of normal stresses in the individual layers of sandwich bar. In this way, designated courses of stresses were compared with the courses of normal stresses in the layers of sandwich designated from a spatial model SOLID45.

In the first loading case, a statically determinate sandwich bar loaded only by the thermal field was considered. This state was achieved by releasing a bond in the common node of Von Mises structure **Fig. 5**, what allowed free movement in the y-axes direction. In Fig. 15, a very good agreement of the axial stresses in the layers of a bar specified by the new bar element and the spatial model SOLID45 for this loading state is seen.

In the second loading case, the case of statically indeterminate bar loaded only by thermal field was considered. This state was achieved by inserting a bond into the common node of Von Mises structure, i.e. by specifying of the global displacement $u_y = 0$. Fig. 16 compares the course of the local displacements u_x of the points on the bar axis designated by a new bar element of homogenized properties and by the spatial model SOLID45. Table 9 summarizes the absolute values of internal forces in terminal nodes in direction of the bar axis determined by the applied models. Fig. 17 illustrates the course of structural

normal stresses in layers, which operate in a sandwich bar in this state of loading. Also, in this case, a very good agreement between the results obtained by one new element and a spatial model can be stated.

In the third loading case, Von Mises structure was stressed by displacement u_y within the range $\langle +L^0 \sin\alpha^0 ; -L^0 \sin\alpha^0 \rangle$ so that to achieve dependence of axial force N or reaction F from displacement u_y during deformation of the structure. The resulting dependence of the axial force N for selected models is presented in the graph in Fig. 19. Table 10 specifies the extreme values of axial force N and reaction F in the common node, which are selected from all the models used in solving this problem. Fig. 20 compares the course of normal stresses in the layers of sandwich bar designated by the new bar element and by the new comparative model SOLID45. Table 12 contains the values of these stresses at the beginning and end of the bar. The presented results correspond to the load step when $\alpha^t = 0°$, i.e. the position when the axial force in the bar reaches the maximum value. Again, a very good agreement of the new approach and the reference solution can be seen. In Table 11, reciprocal differences in the percentage of maximum values of axial forces N and reactions F, which are common to all models less than 0.7%, are seen. That confirms that the designed extended mixing rule is appropriate for the determination of the effective homogenized elastic Young's modulus $E_L^H(x)$.

In the fourth loading case when the rod was loaded up to the moment when the value of the yield stress in the bar was achieved (in the place of the smallest cross-section of the bar), i.e. the bar was still stressed in elastic

area. Besides the structural stress, in such stressed bar, the thermal field was also acted. For this state, Fig. 21 shows the course of displacement of points on the axis of the bar at the stress limit.

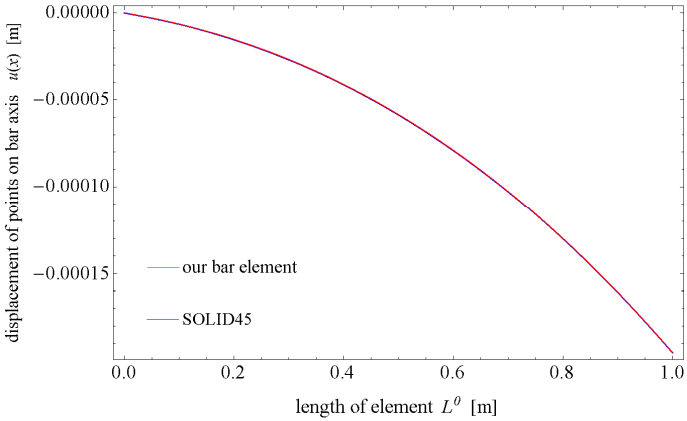

Fig. 21 *Displacement of points on axis of the bar at the stress limit and consideration of thermo-elastic loading*

3. PLANAR BEAM ELEMENT WITH CONSTANT STIFFNESS FOR THE SOLUTIONS OF GEOMETRICALLY NONLINEAR PROBLEMS AND ELASTIC AREA OF LOADING

This part of the study deals with derivation of the finite beam element for the solution of nonlinear problems based on a complete non-incremental formulation. There are prepared the stiffness matrices for planar two node beam element with the closed, constant and symmetric cross-section satisfying Euler-Bernoulli conditions for bending without considering torque transmission.

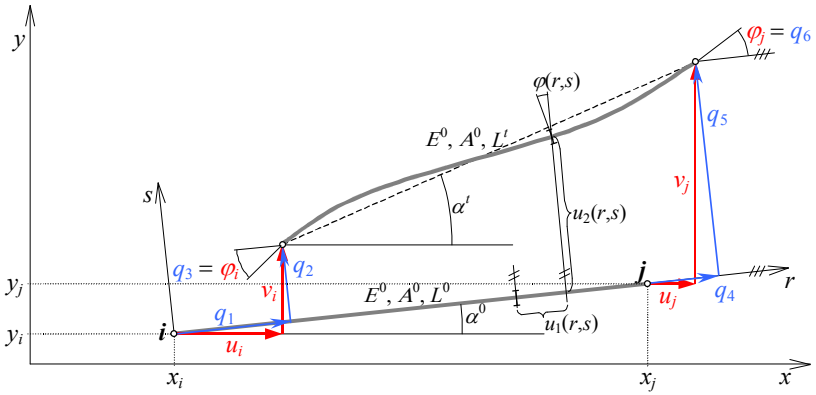

Fig. 22 *Planar beam element in initial configuration and deformed state*

In the derivation of the stiffness matrix of planar beam element, the procedure for formulation of non-incremental geometrically nonlinear FEM equations of equilibrium, which was described in section 1.2 is used.

3.1 Shape functions

A condition for the use of non-linear equilibrium equation [1.6] to compile a local element stiffness matrix is that the displacement of any point of the element is expressed in the form of equation [1.5]. Alternative functions ϕ_{ik} for 2D two node beam element are defined by the linear polynomials for axial displacement and cubic interpolation functions for Hermitean bending displacement components.

For the two-noded planar beam element, the shape function matrix $\mathbf{N}(r,s)$ has a shape known from literature (5, 10, 47). For the displacements of the element points u_1 and u_2 in the direction of the local axis, the matrix of the shape functions can be written in the form

$$\mathbf{N}(r,s)=\begin{bmatrix}\phi_{1k}\\ \phi_{2k}\end{bmatrix}= \\ =\begin{bmatrix} 1-\frac{r}{L^0} & s\left(\frac{6r}{L^{0^2}}-\frac{6r^2}{L^{0^3}}\right) & s\left(-1+\frac{4r}{L^0}-\frac{3r^2}{L^{0^2}}\right) & \frac{r}{L^0} & s\left(-\frac{6r}{L^{0^2}}+\frac{6r^2}{L^{0^3}}\right) & s\left(\frac{2r}{L^0}-\frac{3r^2}{L^{0^2}}\right) \\ 0 & \left(1-\frac{3r^2}{L^{0^2}}+\frac{2r^3}{L^{0^3}}\right) & \left(r-\frac{2r^2}{L^0}+\frac{r^3}{L^{0^2}}\right) & 0 & \left(\frac{3r^2}{L^{0^2}}-\frac{2r^3}{L^{0^3}}\right) & \left(-\frac{r^2}{L^0}+\frac{r^3}{L^{0^2}}\right) \end{bmatrix} \qquad [3.1]$$

In accordance with Fig. 22 the local nodal displacements (or rotations) q_k of the beam element nodal points are defined $\mathbf{q}=[q_k]= \\ =[q_1 \quad q_2 \quad q_3 \quad q_4 \quad q_5 \quad q_6]^{\mathrm{T}}$. Global nodal displacements are arranged in the vector $\mathbf{Q}=[u_i \;\; v_i \;\; \varphi_i \;\; u_j \;\; v_j \;\; \varphi_j]^{\mathrm{T}}$.

In the planar bending of the beam (in the plane determined by local coordinates *r, s*), the displacement vector of arbitrary point of the beam

element is determined by the shape functions [3.1] and the local displacements on nodal points in the relationship

$$\mathbf{u} = \mathbf{N}(r,s)\,\mathbf{q} \qquad [3.2]$$

that we get expressed in the component form by the relationship $u_i = \phi_{ik}\ q_k$

$$\begin{bmatrix} u_1 \\ u_2 \end{bmatrix} = \begin{bmatrix} 1-\frac{r}{L^0} & s\left(\frac{6r}{L^{0^2}}-\frac{6r^2}{L^{0^3}}\right) & s\left(-1+\frac{4r}{L^0}-\frac{3r^2}{L^{0^2}}\right) & \frac{r}{L^0} & s\left(-\frac{6r}{L^{0^2}}+\frac{6r^2}{L^{0^3}}\right) & s\left(\frac{2r}{L^0}-\frac{3r^2}{L^{0^2}}\right) \\ 0 & \left(1-\frac{3r^2}{L^{0^2}}+\frac{2r^3}{L^{0^3}}\right) & \left(r-\frac{2r^2}{L^0}+\frac{r^3}{L^{0^2}}\right) & 0 & \left(\frac{3r^2}{L^{0^2}}-\frac{2r^3}{L^{0^3}}\right) & \left(-\frac{r^2}{L^0}+\frac{r^3}{L^{0^2}}\right) \end{bmatrix} \begin{bmatrix} q_1 \\ q_2 \\ q_3 \\ q_4 \\ q_5 \\ q_6 \end{bmatrix} \qquad [3.3]$$

3.2 Local stiffness matrix of 2D beam element

The transformation relationship between strain and displacement of an arbitrary point of the beam element expressed by derivatives of shape functions $\phi_{ik,r}$ is reduced to a single equation

$$\begin{aligned} \frac{du(r,s)}{dr} &= \phi_{ik,r} q_k = \phi_{1,1}\,q_1 + \phi_{2,1}\,q_2 + \phi_{3,1}\,q_3 + \phi_{4,1}\,q_4 + \phi_{5,1}\,q_5 + \phi_{6,1}\,q_6 = \\ &= \left(-\frac{1}{L^0}\right)q_1 + s\left(\frac{6}{L^{0^2}}-\frac{12r}{L^{0^3}}\right)q_2 + s\left(\frac{4}{L^0}-\frac{6r}{L^{0^2}}\right)q_3 + \left(\frac{1}{L^0}\right)q_4 + s\left(-\frac{6}{L^{0^2}}+\frac{12r}{L^{0^3}}\right)q_5 + s\left(\frac{2}{L^0}-\frac{6r}{L^{0^2}}\right)q_6 \end{aligned} \qquad [3.4]$$

To derive the local stiffness matrix of the two-noded planar beam element according to Fig. 22 the equilibrium relationship [1.6] is used.

From the first member of the equation [1.6] for calculation of the components of linear stiffness matrix, after substitution of $dV = dr\,dA$ and $C_{ijkl} = C_{1111} = E$ we will get relationship

$$K_{nm}^{L} = \frac{1}{4} \int_{L^0} \int_{A^0} E(\phi_{km,l} + \phi_{lm,k})(\phi_{in,j} + \phi_{jn,i}) dA dr \qquad [3.5]$$

For the derivation of the stiffness matrices of the new planar two-noded beam element, the free indices *m* and *n* acquire values to the extent determined by the number of degrees of freedom (displacements) of the element, i.e. for our beam element *m*, *n* = 1 ÷ 6. The result of substituting derivatives of shape functions $\phi_{ik,r}$ [3.4] to [3.5] is the linear stiffness matrix of a planar beam element known from the linear theory. When modifying, we replace integrals by $\int_{A^0} s\, dA = 0$ for the first moment of area and by $\int_{A^0} s^2\, dA = I_Z$ for the second moment of area.

From the second member in [1.6], after substitution *dV* and C_{ijkl} as in case of linear matrix, we modify for the calculation of the components of the first non-linear stiffness matrix

$$K(q)_{nm}^{NL1} = \frac{1}{4} \int_{L^0} \int_{A^0} E \phi_{pm,k}\, \phi_{pr,l} (\phi_{in,j} + \phi_{jn,i})\, q_r\, dA dr \quad . \qquad [3.6]$$

Free indices *m, n* and *r*, for the case of the derivation of the new planar two nodal beam element acquire values in the range 1 ÷ 6. Substituting derivatives of shape functions into [3.6] and the necessary modifications in the derived equations result in the integrals for calculation of higher-order

moments of area: third moment of area $\int_{A^0} s^3\, dA = I_{Z2}$. For symmetrical cross-sections, however, $I_{Z2} = 0$ is valid.

From the third member of equation [1.6] after substitution of dV and C_{ijkl} for the calculation of components of the second non-linear stiffness matrix, we obtain

$$K(q)_{nm}^{NL2} = \frac{1}{2} \int_{L^0} \int_{A^0} E \phi_{pr,i}\, \phi_{pn,j} (\phi_{km,l} + \phi_{lm,k})\, q_r\, dA dr \ . \qquad [3.7]$$

In this case, in the derived equations, an integral to calculate third moment of area will occur.

By substituting derivatives of shape functions into the last integral in [1.6] and after substitution of dV and C_{ijkl} we get equation for calculation of the components of the second nonlinear stiffness matrix.

$$K(q)_{nm}^{NL3} = \frac{1}{2} \int_{L^0} \int_{A^0} E \phi_{pm,k}\, \phi_{pv,l}\, \phi_{rq,i}\, \phi_{rn,j}\, q_v\, q_q\, dA dr \qquad [3.8]$$

Necessary modifications in derived equations result in integrals for calculation of high order moments of area: third moment of area $\int_{A^0} s^3\, dA = I_{Z2} = 0$ (for the symmetric cross sections) and bi-quadratic moment of area $\int_{A^0} s^4\, dA = I_{Z3}$. Total local stiffness matrix of two nodal planar beam element is determined by the sum [1.8] of the components derived from the relations [3.5], [3.6], [3.7] and [3.8]. The resulting local

stiffness matrix of planar non-linear beam element, like all its components is symmetrical.

In previous terms the bi-quadratic moment of area I_{Z3} for circular and rectangle cross-section is expressed

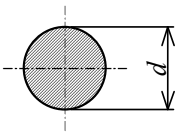

$$I_{Z3} = \frac{\pi d^6}{512}$$

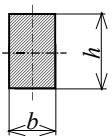

$$I_{Z3} = \frac{b h^5}{80}$$

3.3 Local stiffness matrix of beam element in the shape invariant to rigid motion

During the deformation process, the large rotations of the element occur, which causes rotation of the local beam axis *r* between the deformation steps (iterations) as is shown in Fig. 23.

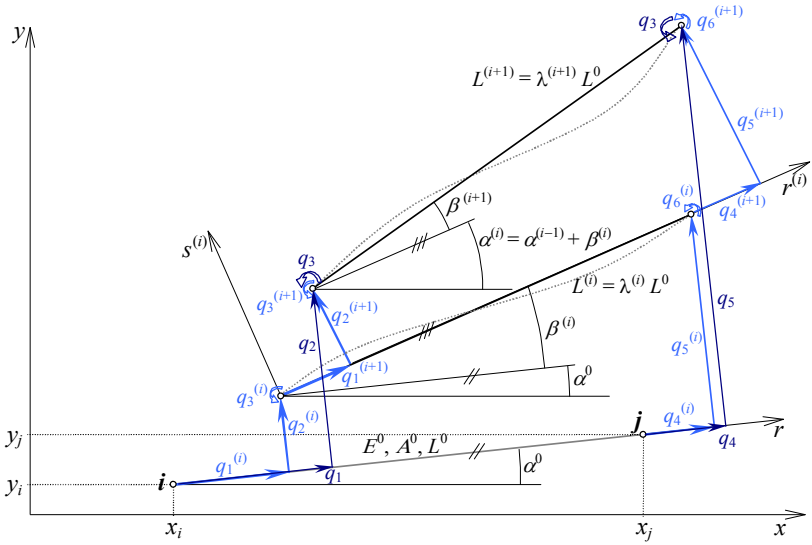

Fig. 23 *Local displacements of element end nodes in different deformation states (iterations)*

For the iterative solution in seeking an equilibrium of the internal and external forces, $q_i^{(i)}$ are local increments of the displacements related to the current local coordinate system of the deformed element ($r^{(i)}$, $s^{(i)}$) with the angle $\alpha^t = \alpha^{(i)}$ with the respect to the x-axis of the global coordinate system. The resulting node displacements after the exact solution are determined by the total local displacements q_k, which are related to the initial configuration, when a local coordinate system of un-deformed element (r,s) is rotated given the global axis x by angle α^0. Total nodal rotations q_3 or q_6

are given by the sum $q_3 = \sum_{j=1}^{n} q_3^{(i)}$ $q_6 = \sum_{j=1}^{n} q_6^{(i)}$, where n is number of iterations.

As in the case of non-linear bar elements also to derive the beam element stiffness matrix **K**(**q**) [3.9], it is necessary to know the local displacements of the element end nodes. To transform the global nodal displacements to the local displacements, classical transformational relationship known from linear theory cannot be used, because the transformation law ignores rigid rotation. In the case of planar problem solution, the large-rotation problem for displacements in the direction of the local longitudinal axis of the element r (node joints) can be solved similarly to the bar element, by implementation of the dimensionless, i.e. rigid displacement (rotation) invariant variable stretching λ [2.14], which can be determined also from the global displacements of the element nodes (valid length of the node joints). Displacements in the direction of the local axis s can be replaced by the angle of rotation of the joint of the nodal points of the beam element β in valid configuration with regard to the last known configuration of the element assuming that deformation in the axis of the bar is caused only by the stress from axial force N.

$$\lambda = \frac{L^t}{L^0} = 1 + \frac{q_4 - q_1}{L^0} \quad \text{and} \quad \tan\beta = \frac{q_5 - q_2}{L^t} = \frac{q_5 - q_2}{\lambda L^0} \qquad [3.9]$$

of which can be expressed

$$q_4 - q_1 = (\lambda - 1)L^0 \quad \text{and} \quad q_5 - q_2 = \lambda L^0 \tan\beta \qquad [3.10]$$

In the case of stiffness matrices derivation of spatial beam element, for transformation from a global to a local coordinate system, Rodrigues formula (76) can be used.

The resulting total local stiffness matrix of beam element invariant to rigid body motion, after the introduction of dimensionless values [3.9] and relevant modifications has the shape

$$\mathbf{K} = \begin{bmatrix} K_{11} & K_{12} & K_{13} & -K_{11} & -K_{12} & K_{16} \\ & K_{22} & K_{23} & -K_{12} & -K_{22} & K_{26} \\ & & K_{33} & -K_{13} & -K_{13} & K_{36} \\ & & & K_{11} & K_{12} & -K_{16} \\ & sym. & & & K_{22} & -K_{26} \\ & & & & & K_{66} \end{bmatrix} \qquad [3.11]$$

where the terms of the resulting invariant local stiffness matrix are equal to

$$K_{11} = \frac{AE}{L^0}\left(1 + \frac{3}{2}(\lambda - 1) + \frac{1}{2}(\lambda - 1)^2\right) +$$

$$+ \frac{2I_Z E}{(L^0)^3}\left(3\lambda^2(\tan\beta)^2 - 3\lambda\tan\beta(q_3 + q_6) + (q_3^2 + q_3 q_6 + q_6^2)\right)$$

$$K_{12} = \frac{3I_Z E}{(L^0)^3}(2\lambda + 1)\left(2\lambda\tan\beta(q_3 + q_6)\right)$$

$$K_{13} = \frac{I_Z E}{(L^0)^2}(2\lambda + 1)\left(2\lambda\tan\beta(2q_3 + q_6)\right)$$

$$K_{16} = \frac{I_Z E}{(L^0)^2}(2\lambda + 1)\left(2\lambda\tan\beta(q_3 + 2q_6)\right)$$

$$K_{22} = \frac{12I_Z E}{(L^0)^3}\left(1 + \frac{3}{2}(\lambda - 1) + \frac{1}{2}(\lambda - 1)^2\right) +$$

$$+ \frac{24I_{Z3} E}{5(L^0)^5}\left(27\lambda^2(\tan\beta)^2 - 27\lambda\tan\beta(q_3 + q_6) + (8q_3^2 + 11q_3 q_6 + 8q_6^2)\right)$$

$$K_{23} = \frac{6I_Z E}{(L^0)^2}\left(1+\frac{3}{2}(\lambda-1)+\frac{1}{2}(\lambda-1)^2\right)+$$
$$+\frac{6I_{Z3} E}{5(L^0)^4}\left(54\lambda^2(\tan\beta)^2-4\lambda\tan\beta(16q_3+11q_6)+(21q_3^2+22q_3q_6+11q_6^2)\right)$$

$$K_{26} = \frac{6I_Z E}{(L^0)^2}\left(1+\frac{3}{2}(\lambda-1)+\frac{1}{2}(\lambda-1)^2\right)+$$
$$+\frac{6I_{Z3} E}{5(L^0)^4}\left(54\lambda^2(\tan\beta)^2-4\lambda\tan\beta(11q_3+16q_6)+(11q_3^2+22q_3q_6+21q_6^2)\right)$$

$$K_{33} = \frac{4I_Z E}{L^0}\left(1+\frac{3}{2}(\lambda-1)+\frac{1}{2}(\lambda-1)^2\right)+$$
$$+\frac{4I_{Z3} E}{5(L^0)^3}\left(48\lambda^2(\tan\beta)^2-3\lambda\tan\beta(21q_3+11q_6)+(22q_3^2+19q_3q_6+7q_6^2)\right)$$

$$K_{36} = \frac{2I_Z E}{L^0}\left(1+\frac{3}{2}(\lambda-1)+\frac{1}{2}(\lambda-1)^2\right)+$$
$$+\frac{2I_{Z3} E}{5(L^0)^3}\left(66\lambda^2(\tan\beta)^2-66\lambda\tan\beta(q_3+q_6)+(19q_3^2+28q_3q_6+19q_6^2)\right)$$

$$K_{66} = \frac{4I_Z E}{L^0}\left(1+\frac{3}{2}(\lambda-1)+\frac{1}{2}(\lambda-1)^2\right)+$$
$$+\frac{4I_{Z3} E}{5(L^0)^3}\left(48\lambda^2(\tan\beta)-3\lambda\tan\beta(11q_3+21q_6)+(7q_3^2+19q_3q_6+22q_6^2)\right)$$

3.4 Local vector of internal nodal forces

Local vector of internal nodal forces $\mathbf{F}^{int}(\mathbf{q})$ that can be obtained from the equilibrium non-linear equation $\mathbf{K}(\mathbf{q})\,\mathbf{q} = \mathbf{F}$ by multiplying the local non-linear stiffness matrix $\mathbf{K}(\mathbf{q})$ [3.9] by vector of valid local displacements $\mathbf{q}$ or

from equation $\mathbf{F}^{int} = \mathbf{K}\,\mathbf{q}$ where the matrix $\mathbf{K}$ is given by expression [3.11], can be expressed in invariant form

$$\mathbf{F}^{int} = \begin{bmatrix} -K_{11}(\lambda-1)L^0 - K_{12}\,\lambda\,L^0\tan\beta + K_{13}\,q_3 + K_{16}q_6 \\ -K_{12}(\lambda-1)L^0 - K_{22}\,\lambda\,L^0\tan\beta + K_{23}\,q_3 + K_{26}\,q_6 \\ -K_{13}(\lambda-1)L^0 - K_{23}\,\lambda\,L^0\tan\beta + K_{33}\,q_3 + K_{36}q_6 \\ K_{11}(\lambda-1)L^0 + K_{12}\,\lambda\,L^0\tan\beta - K_{13}\,q_3 - K_{16}q_6 \\ K_{12}(\lambda-1)L^0 + K_{22}\,\lambda\,L^0\tan\beta - K_{23}\,q_3 - K_{26}q_6 \\ -K_{16}(\lambda-1)L^0 - K_{26}\lambda\,L^0\tan\beta + K_{36}\,q_3 + K_{66}\,q_6 \end{bmatrix} \qquad [3.12]$$

where K_{11} to K_{66} are identical to the elements of the stiffness matrix [3.11].

3.5 Local tangential stiffness matrix of 2D beam element

To accelerate the convergence of the nonlinear equation system solution, in the case of using Newton-Rapson method is advisable to use tangential element stiffness matrix.

To determine the members of the local tangential stiffness matrix of the new beam element, the relation [1.9] can be used. Another option is the compilation of a tangential stiffness matrix of beam element using the derivative of the potential energy of internal forces by local nodal displacements (Castigliano principle).

Potential energy of internal forces in the current configuration for the complete non-incremental formulation can be expressed by (42, 47, 48)

$$A = \frac{1}{2} \int_{V^0} S_{ij} \, E_{ij} \, dV \qquad [3.13]$$

while integration is underway through the initial volume of the element. Assuming that the isotropic tensor of material properties is constant throughout the entire deformation process, the 2nd Piola-Kirchhoff stress tensor $S_{ij} = C_{ijkl} \, E_{kl} = C_{ijkl}(e_{kl} + \eta_{kl})$ can be expressed by components of Green-Lagrange strain tensor [1.2]. Potential energy of internal forces are expressed by the relationship

$$\begin{aligned} A &= \frac{1}{2} \int_{V^0} C_{ijkl}(e_{kl} + \eta_{kl})(e_{ij} + \eta_{ij}) \, dV = A^L + A^{NL} = \\ &= \frac{1}{2} \int_{V^0} C_{ijkl} \, e_{kl} \, e_{ij} \, dV + \frac{1}{2} \int_{V^0} C_{ijkl}(e_{kl} \, \eta_{ij} + \eta_{kl} \, e_{ij} + \eta_{kl} \, \eta_{ij}) \, dV \end{aligned} \qquad [3.14]$$

Members of the local tangential element stiffness matrix $\mathbf{K}^T = [K^T_{mn}]$ can be obtained by derivation of the potential energy of internal forces according to the nodal displacements q_k in the form

$$K^T_{mn} = \frac{\partial^2 A}{\partial q_m \partial q_n} = K^L_{mn} + K^{NLT}_{mn} = \frac{\partial^2 A^L}{\partial q_m \partial q_n} + \frac{\partial^2 A^{NL}}{\partial q_m \partial q_n} \quad . \qquad [3.15]$$

where members K^L_{mn} form linear component $\mathbf{K}^L$ and members K^{NL}_{mn} form nonlinear component $\mathbf{K}^{NL}$ of the total local stiffness matrix of element $\mathbf{K}$.

In the case of two-node planar beam element, the non-linear transformational relationship between strain and displacement of nodes is reduced to one component of the Green-Lagrange strain tensor

$$E_{11} = e_{11} + \eta_{11} = u_{1,1} + \frac{1}{2}\left(u_{1,1}\, u_{1,1}\right) \qquad [3.16]$$

where the derivative of displacements $u_{1,1}$ is expressed by relationship [3.4]. By the derivation of the linear component of internal potential energy A^L according to local displacements q_k and after substitution $dV = dr\ dA$ and $C_{1111} = E$ we obtain the expression for calculation the elements of linear components of the local tangent stiffness matrix of one-dimensional element

$$K_{mn}^{L} = \frac{\partial^2}{\partial q_m \partial q_n}\left[\frac{E}{2}\int_{V^0}(u_{1,1})^2\, dV\right] = E\int_{L^0}\int_{A^0}\frac{\partial u_{1,1}}{\partial q_m}\frac{\partial u_{1,1}}{\partial q_n}\, dA\, dr \qquad [3.17]$$

Similarly, but from the derivation of the first and second members of nonlinear component of the potential energy A^{NL} and after relevant modifications, we obtain relations for calculating the members of two non-linear components of tangential stiffness matrix of one-dimensional element

$$K_{mn}^{NLT1} = \frac{\partial^2}{\partial q_m \partial q_n}\left[E\int_{V^0} e_{11}\,\eta_{11}\, dV\right] = 3E\int_{L^0}\int_{A^0} u_{1,1}\frac{\partial u_{1,1}}{\partial q_m}\frac{\partial u_{1,1}}{\partial q_n}\, dA\, dr \qquad [3.18]$$

$$K_{mn}^{NLT2} = \frac{\partial^2}{\partial q_m \partial q_n}\left[\frac{E}{2}\int_{V^0}\eta_{11}^2\, dV\right] = \frac{3}{2}E\int_{L^0}\int_{A^0} u_{1,1}^2\frac{\partial u_{1,1}}{\partial q_m}\frac{\partial u_{1,1}}{\partial q_n}\, dA\, dr \quad . \qquad [3.19]$$

The local full non-linear tangential stiffness matrix of the two-node planar beam element is given by the sum of the linear and non-linear sub-matrices

$$\mathbf{K}^T(\mathbf{q}) = \mathbf{K}^L + \mathbf{K}(\mathbf{q})^{NLT1} + \mathbf{K}(\mathbf{q})^{NLT2} \qquad [3.20]$$

3.6 Local tangential stiffness matrix of beam element expressed in the form invariant to rigid body motion

Fig. 24 shows deformation states of the beam element in individual iteration steps. As mentioned in section 3.3 it is not possible for the calculation of local tangential stiffness matrix $\mathbf{K}^T(\mathbf{q})$ defined by the relationship [3.20] to use local displacements q_k, because they cannot be derived from the global displacements due to the effect of large rotations.

Because in the iteration process, the global displacements vector $\mathbf{Q}$ is determined, it is necessary to replace the local displacements q_k by variables invariant to rigid body motion (rotation) - stretching λ and angle β of the rotations of the beam element end node joints defined by the relationship [3.9].

After substituting relations [3.10] for calculating non-linear relationship of the local tangential components of the stiffness matrix [3.17], [3.18] and [3.19], the total local non-linear tangential stiffness matrix [3.20] can be expressed in the form invariant to rigid motion

$$\mathbf{K}^T = \begin{bmatrix} K_{11}^T & K_{12}^T & K_{13}^T & -K_{11}^T & -K_{12}^T & K_{16}^T \\ & K_{22}^T & K_{23}^T & -K_{12}^T & -K_{22}^T & K_{26}^T \\ & & K_{33}^T & -K_{13}^T & -K_{23}^T & K_{36}^T \\ & & & K_{11}^T & K_{12}^T & -K_{16}^T \\ & \textit{sym.} & & & K_{22}^T & -K_{26}^T \\ & & & & & K_{66}^T \end{bmatrix} \qquad [3.21]$$

where

$$K_{11}^{T} = \frac{AE}{L^0}\left(1+3(\lambda-1)+\frac{3}{2}(\lambda-1)^2\right)+$$
$$+\frac{26I_Z E}{(L^0)^3}\left(3\lambda^2(\tan\beta)^2-3\lambda\tan\beta(q_3+q_6)+(q_3^2+q_3 q_6+q_6^2)\right)$$
$$K_{12}^{T} = \frac{18I_Z E}{(L^0)^3}(2\lambda+1)\left(2\lambda\tan\beta(q_3+q_6)\right)$$
$$K_{13}^{T} = \frac{6I_Z E}{(L^0)^2}(2\lambda+1)\left(2\lambda\tan\beta(2q_3+q_6)\right)$$
$$K_{16}^{T} = \frac{6I_Z E}{(L^0)^2}(2\lambda+1)\left(2\lambda\tan\beta(q_3+2q_6)\right)$$
$$K_{22}^{T} = \frac{12I_Z E}{(L^0)^3}\left(1+3(\lambda-1)+\frac{3}{2}(\lambda-1)^2\right)+$$
$$+\frac{72I_{Z3} E}{5(L^0)^5}\left(27\lambda^2(\tan\beta)^2-27\lambda\tan\beta(q_3+q_6)+(8q_3^2+11q_3 q_6+8q_6^2)\right)$$
$$K_{26}^{T} = \frac{6I_Z E}{(L^0)^2}\left(1+3(\lambda-1)+\frac{3}{2}(\lambda-1)^2\right)+$$
$$+\frac{6I_{Z3} E}{5(L^0)^4}\left(54\lambda^2(\tan\beta)^2-4\lambda\tan\beta(11q_3+16q_6)+(11q_3^2+22q_3 q_6+21q_6^2)\right)$$
$$K_{23}^{T} = \frac{6I_Z E}{(L^0)^2}\left(1+3(\lambda-1)+\frac{3}{2}(\lambda-1)^2\right)+$$
$$+\frac{18I_{Z3} E}{5(L^0)^4}\left(54\lambda^2(\tan\beta)^2-4\lambda\tan\beta(16q_3+11q_6)+(21q_3^2+22q_3 q_6+11q_6^2)\right)$$

$$K_{33}^T = \frac{4I_Z E}{L^0}\left(1+3(\lambda-1)+\frac{3}{2}(\lambda-1)^2\right)+$$
$$+\frac{12I_{Z3}E}{5(L^0)^3}\left(48\lambda^2(\tan\beta)^2-3\lambda\tan\beta(21q_3+11q_6)+(22q_3^2+19q_3q_6+7q_6^2)\right)$$
$$K_{36}^T = \frac{2I_Z E}{L^0}\left(1+3(\lambda-1)+\frac{3}{2}(\lambda-1)^2\right)+$$
$$+\frac{6I_{Z3}E}{5(L^0)^3}\left(66\lambda^2(\tan\beta)^2-66\lambda\tan\beta(q_3+q_6)+(19q_3^2+28q_3q_6+19q_6^2)\right)$$
$$K_{66}^T = \frac{4I_Z E}{L^0}\left(1+3(\lambda-1)+\frac{3}{2}(\lambda-1)^2\right)+$$
$$+\frac{12I_{Z3}E}{5(L^0)^3}\left(48\lambda^2(\tan\beta)^2-3\lambda\tan\beta(11q_3+21q_6)+(7q_3^2+19q_3q_6+22q_6^2)\right)$$

The resulting local tangential stiffness matrix of planar non-linear beam element is as symmetrical as all its components.

3.7 Algorithm for solving problems with new non-linear beam element loaded in elastic area

The procedure for solving the problem of non-linear deformation of the structure consisting of the new nonlinear beam element is identical to the procedure described in section 2.1.4. Changes, comparing those being already described for nonlinear bar element, are summarized in the following subsections. To calculate global displacements (rotations) on nodal points of the element from the global non-linear equilibrium equations, the Newton's iteration method and non-linear tangential stiffness matrix $\mathbf{K}^T$ [3.21] is used. Internal forces (moments) in the beam cannot be calculated from the global stiffness relationship due to the effect of large

rotation. In order to eliminate the problems associated with the transformation of the internal forces from the global to the local coordinate system, for calculation of internal forces we will use a local non-linear stiffness matrix **K** [3.11] invariant to the rigid motion (rotation) of the beam. The local vector of internal forces $\mathbf{F}^{\text{int}}$ will then have a shape defined by the relationship [3.12].

3.7.1 Computation of initial global displacements of the system

The beginning of the solution requires calculation of initial values of global displacements for non-linear calculation. It is usually based on local linear stiffness matrix $\mathbf{K}^L$, which is transformed into a global system according to a relationship for one element

$$\mathbf{K}^G = \mathbf{T}_0^{\mathrm{T}}\, \mathbf{K}^L\, \mathbf{T}_0 \,. \qquad [3.22]$$

where the transformation matrix $\mathbf{T}_0$ depends on the angle α^0 of the element axis in the initial configuration. In the next step, the stiffness matrix of the whole system $\mathbf{K}_{\text{cel}}^G$ is prepared and similarly a vector of external load of the whole system $\mathbf{F}_{\text{cel}}^G$ is designed. Initial global displacements $\mathbf{Q}^0$

$$\mathbf{Q}^0 = \begin{bmatrix} u_i & v_i & \varphi_i & u_j & v_j & \varphi_j \end{bmatrix}^{\mathrm{T}} . \qquad [3.23]$$

are determined from the linear equilibrium relationship

$$\mathbf{K}_{\text{cel}}^G\, \mathbf{Q}^0 = \mathbf{F}_{\text{cel}}^G \,. \qquad [3.24]$$

3.7.2 Iterative calculation of global displacements from nonlinear system of equations

The increment of global nodal displacements $\Delta\mathbf{Q}$ in the i^{th} iteration is calculated using non-linear global tangential stiffness matrix and global residual force vector

$$\mathbf{K}_{T\text{cel}}^{G}\,\Delta\mathbf{Q} = \mathbf{F}_{\text{cel}}^{G\text{res}} \quad . \qquad [3.25]$$

where $\mathbf{F}_{\text{cel}}^{G\text{res}}$ is the vector of global residual (loss) forces (section 3.7.3) and $\mathbf{K}_{T\text{cel}}^{G}$ is the total tangential matrix of the system structure prepared from extended global tangential stiffness matrix of elements $\mathbf{K}_{T}^{G}$. Non-linear global tangential stiffness matrix of an element $\mathbf{K}_{T}^{G}$ can be expressed by the classical transformation using transformation matrix $\mathbf{T}$ from the local nonlinear tangential stiffness matrix $\mathbf{K}^{T}$ [3.21]

$$\mathbf{K}_{T}^{G} = \mathbf{T}^{\mathrm{T}}\,\mathbf{K}^{T}\,\mathbf{T} \quad . \qquad [3.26]$$

For the two-node beam element stressed in a plane, the matrix $\mathbf{T}$ has the form known from literature (9)

$$\mathbf{T} = \begin{bmatrix} \cos\alpha^t & \sin\alpha^t & 0 & 0 & 0 & 0 \\ -\sin\alpha^t & \cos\alpha^t & 0 & 0 & 0 & 0 \\ 0 & 0 & 1 & 0 & 0 & 0 \\ 0 & 0 & 0 & \cos\alpha^t & \sin\alpha^t & 0 \\ 0 & 0 & 0 & -\sin\alpha^t & \cos\alpha^t & 0 \\ 0 & 0 & 0 & 0 & 0 & 1 \end{bmatrix}, \qquad [3.27]$$

where α^t is the angle determining rotation of the joint of terminal nodes of the beam element in valid configuration, which is a function of current coordinates of the nodal points of element $\{[X_i, Y_i], [X_j, Y_j]\}$ and valid length L^t.

In accordance with Fig. 24 we can express the total angle α of rotation of the element nodal joints in the current configuration of the beam considering the global axis x. The angle is defined as the sum of $\alpha^t = \alpha^{(i-1)} + \beta^{(i)}$, where $\beta^{(i)}$ is the increment of the rotational angle of nodal joints in the current iteration due to the position of the nodal joints of the beam in the previous known configuration.

The overall angle of rotation can be determined using the sum of the angles of rotations of the node joints in all performed iterations, i.e. $\alpha^t = \alpha^0 + \sum\beta^{(i)}$, where α^0 is rotation angle of the beam axis in undeformed, initial configuration in relation to axis x of the global coordinate system.

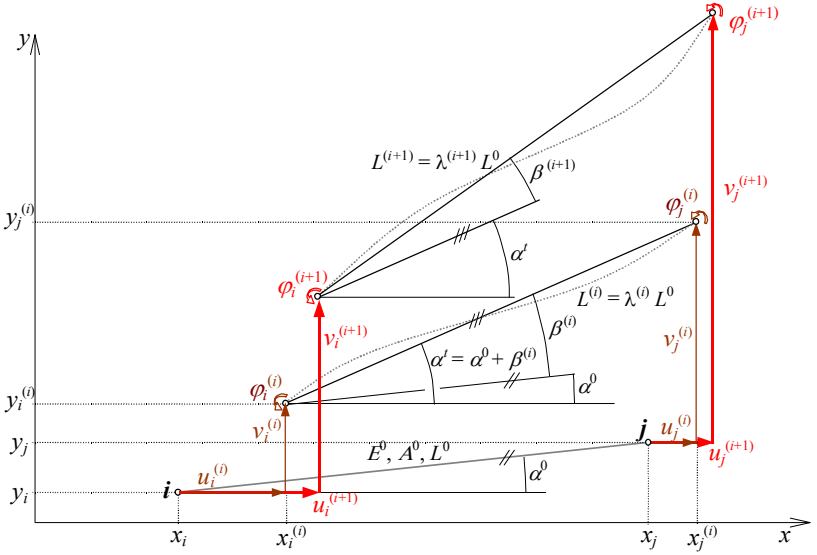

Fig. 24 *Changing global displacements during an iterative process*

3.7.3 Vector of global internal forces

Vector of local internal forces and moments $\mathbf{F}^{\text{int}} = \begin{bmatrix} N_i & T_i & M_i & N_j & T_j & M_j \end{bmatrix}^{\text{T}}$ has, in the case of the new the beam element, the shape given by vector [3.12]. f the vector of local internal forces in the bar is expressed by stretching λ and angle of rotation of the nodal joint β defined in the form [3.9], the global internal forces and moments can be obtained by standard transformation using transposed transformation matrix **T** for the beam element

$$\mathbf{F}^{G\,\mathrm{int}} = \mathbf{T}^{\mathrm{T}}\,\mathbf{F}^{\mathrm{int}}\,. \qquad [3.28]$$

Vector of global internal forces for two-noded beam element in a two-dimensional space has the form

$$\mathbf{F}^{G\,\mathrm{int}} = \left[F_{Xi}^{G\,\mathrm{int}} \quad F_{Yi}^{G\,\mathrm{int}} \quad M_{Zi}^{G\,\mathrm{int}} \quad F_{Xj}^{G\,\mathrm{int}} \quad F_{Yj}^{G\,\mathrm{int}} \quad M_{Zj}^{G\,\mathrm{int}}\right]^{\mathrm{T}}. \qquad [3.29]$$

By the sum of extended vectors of global internal forces, we obtain the vector of total global nodal forces of the system $\mathbf{F}_{\mathrm{cel}}^{G\,\mathrm{int}}$, which represents the exact nodal forces (moments) corresponding to the valid deformation of beam element.

Global residual force vector $\mathbf{F}_{\mathrm{cel}}^{G\mathrm{res}}$ can then be expressed as the difference between external global load vector $\mathbf{F}_{\mathrm{cel}}^{G\mathrm{ext}}$ and the total internal global nodal forces $\mathbf{F}_{\mathrm{cel}}^{G\,\mathrm{int}}$ of the system

$$\mathbf{F}_{\mathrm{cel}}^{G\mathrm{res}} = \mathbf{F}_{\mathrm{cel}}^{G\mathrm{ext}} - \mathbf{F}_{\mathrm{cel}}^{G\,\mathrm{int}}\,. \qquad [3.30]$$

To determine the accuracy of the iterative procedure we use Euclidean norm of residual forces

$$\left\|\mathbf{F}_{\mathrm{cel}}^{G\mathrm{res}}\right\| = \sqrt{\mathbf{F}_{\mathrm{cel}}^{G\mathrm{res}}.\mathbf{F}_{\mathrm{cel}}^{G\mathrm{res}}}\,, \qquad [3.31]$$

that we compare to the norm of external loading forces $\left\|\mathbf{F}_{\mathrm{cel}}^{G\mathrm{ext}}\right\|$. Completion of the iteration process occurs after fulfilling the condition

$$\left\|\mathbf{F}_{\mathrm{cel}}^{G\mathrm{res}}\right\| \le \varepsilon \left\|\mathbf{F}_{\mathrm{cel}}^{G\mathrm{ext}}\right\|\,, \qquad [3.32]$$

where ε specifies the tolerance (accuracy) of the equilibrium achievement.

The total global displacement after the i^{th} iteration is then

$$\mathbf{Q}^i = \mathbf{Q}^{i-1} + \Delta\mathbf{Q} \,. \qquad [3.33]$$

3.8 Numerical experiment

To assess the accuracy and effectiveness of the new nonlinear beam element, the problem of deflection of statically definite cantilever beam with a length L^0, of the constant full circular cross-section according to Fig. 25 with loading in elastic area was solved. The results of the analysis were compared with the reference results obtained by solving the problem using models developed in the commercial software ANSYS:

- BEAM3 model – one-dimensional model with dividing elements to the selected number of finite elements BEAM3. Cross-sectional characteristics corresponded to the full circular cross section with a diameter according to the assignment of the solved model. Boundary conditions matched the problem solution.
- SOLID45 model – spatial model consisting of 5100 body elements SOLID45 creating a cylinder $\varnothing d - L^0$ with the dimensions according to assignment of the solved problem.

The input parameters for the problem solution: elasticity modulus $E = 200$ GPa, $L^0 = 1\,000$ mm, diameter $d = 20$ mm, cross-sectional area $A = 314{,}159$ mm^2, $I_Z = 7\,853{,}98$ mm^4, $I_{Z3} = 392\ \ 699$ mm^6. The beam is loaded by conservative vertical force $F = 1000$ N.

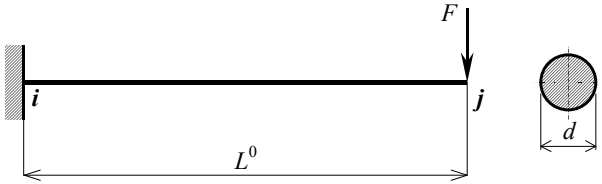

Fig. 25 *Cantilever beam with an end point load*

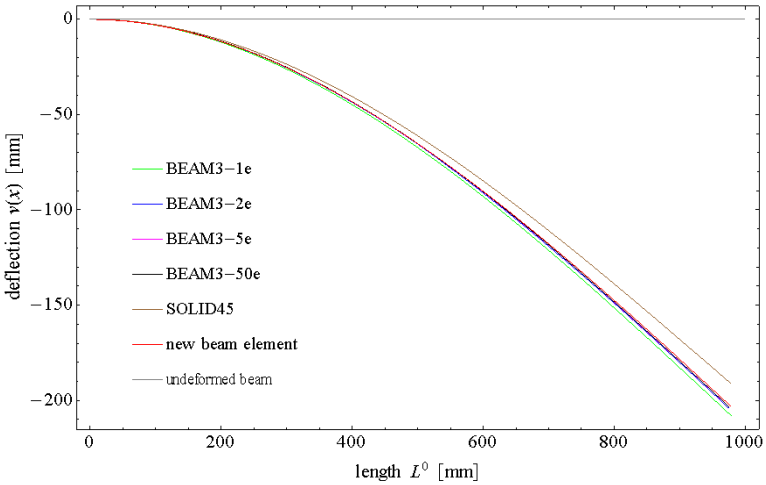

Fig. 26 *Deflection of beam for different models*

THE RESULTING VALUES OF DISPLACEMENTS AND ROTATIONS IN THE BEAM ENDPOINT OBTAINED BY THE NEWLY DEVELOPED BEAM ELEMENT AND THE REFERENCE SOLUTIONS BY THE CODE ANSYS

Table 13

	u_{xj} [mm]	v_{yj} [mm]	φ_{zj} [rad]
BEAM3 – 1 element	–20.530	–208.298	–0.314385
BEAM3 – 2 elements	–24.054	–204.390	–0.309077
BEAM3 – 5 elements	–24.952	–203.343	–0.307611
BEAM3 – 10 elements	–25.077	–203.197	–0.307403
BEAM3 – 50 elements	–25.117	–203.150	–0.307336
BEAM3 – 100 elements	–25.118	–203.149	–0.307334
SOLID model	–22.170	–191.039	–0.288660
our beam – 1 element	–20.911	–203.425	–0.311654
our beam – 2 elements	–23.030	–200.260	–0.308628
our beam – 5 elements	–23.888	–199.474	–0.307962
our beam – 10 elements	–24.019	–199.371	–0.307874

REACTIONS IN THE BEAM CONSTRAIN OBTAINED USING THE DEVELOPED BEAM ELEMENT AND THE REFERENCE SOLUTIONS

Table 14

	R_x [N]	R_y [N]	M_z [Nmm]	*iter.*
BEAM3 – 1 element	$-0.63121\ 10^{-4}$	1 000	987 670	7
BEAM3 – 2 elements	$-0.54046\ 10^{-5}$	1 000	978 420	9
BEAM3 – 5 elements	$-0.12746\ 10^{-5}$	1 000	975 460	9
BEAM3 – 10 elements	$0.26962\ 10^{-5}$	1 000	975 020	8
BEAM3 – 50 elements	$0.12556\ 10^{-5}$	1 000	974 880	6
BEAM3 – 100 elements	$0.85225\ 10^{-7}$	1 000	974 880	7
our beam – 1 element	$0.172273\ 10^{-4}$	1 000	979 090	8
our beam – 2 elements	$0.605573\ 10^{-4}$	1 000	976 971	9
our beam – 5 elements	$0.620974\ 10^{-5}$	1 000	976 114	9
our beam – 10 elements	$0.311687\ 10^{-5}$	1 000	975 983	9

Summary of results

Based upon the results of the point displacements at the free end of the cantilever beam listed in Table 13, as well as from the process of deformation of particular models in Fig. 26, it can be concluded that the deformations determined by one new non-linear beam element are comparable with the results from a model consisting of minimum five beam elements BEAM3. Fig. 27 shows that by increasing mesh density of the model with the new beam element, the results of deformation are getting closer to the solution obtained from the deformation of spatial model SOLID45.

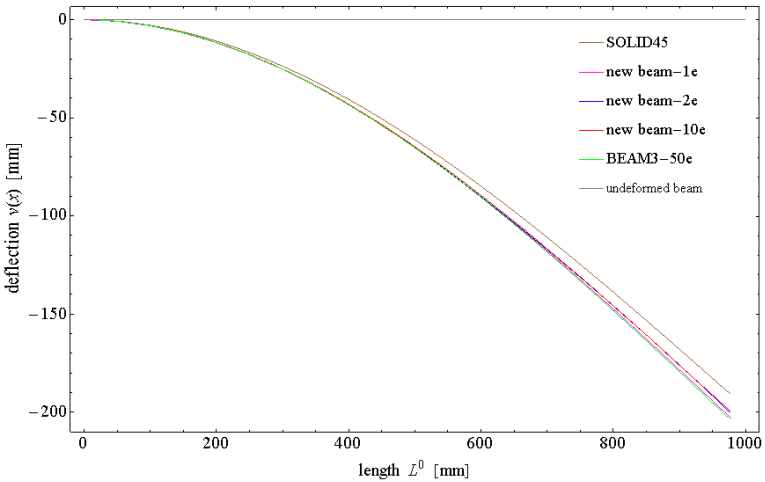

Fig. 27 *Comparison of deflection of models with the new beam elements and different mesh density*

Significant agreement of the results obtained from the spatial model and the derived beam elements can be achieved by the use of two new elements.

Even when using a model with 100 elements BEAM3, there was not such an agreement of the results obtained. The results of deformation calculated by one new element are comparable to traditional solutions for hermitian element BEAM3 divided into 50 elements, considerable deviation occurs only in the value of displacement in the direction of the global x-axis. Table 14 gives the reaction values derived from the used models. The difference between the value of the moment M_z in relation specified by one new beam element and for the model with 100 elements BEAM3 is 0.432% and for the model with ten new beam elements, the deviation moments is reduced to 0.113%. This difference is caused by the fact that the results of deformation in the direction of the global x-axis calculated by models with the new element are smaller than those obtained by the models with BEAM3 elements. Displacements defined by the new element are in better agreement with the results from the spatial model SOLID45.

The number of iterations needed to obtain results by the models with new beam element at a standard accuracy in ANSYS programme was comparable. To achieve comparable results, a model with fewer new elements is needed. It can be stated that the new nonlinear beam element achieves greater efficiency and accuracy.

The new element makes it possible to solve problems of deformation of frame structures by using fewer elements, and in some cases with its help there will be possible to solve problems using the procedure "*one bar = one finite element*". Differences in the size of deformation specified by the beam models (by new beam elements or traditional element BEAM3), and the

model SOLID45 with body elements of the spatial stress is particularly in incomplete agreement of both FEM physical models.

CONCLUSIONS

This monograph is devoted to derivation and application of non-linearized stiffness matrices of one-dimensional elements for the solution of geometrically non-linear problems based on complete geometrically non-linear non-incremental formulation described in section 1.2.

In the first part, the stiffness matrices of geometrically non-linear bar element of variable stiffness are derived. In designing of stiffness matrices, the expanded concept of transfer functions and constants allowing exact inclusion of continuous variability of the cross-section and the material properties was used. On this basis, the stiffness matrices of bar elements of variable cross sections loaded in an elastic area were derived.

The non-linear bar element is extended in implementation of variability of material properties and the possibility of loading the bar in elasto-plastic area. To assess the non-linear behaviour of the structure, the problem of deformation of Mises structure was selected. The results of numerical experiments obtained by new elements are compared with those obtained by conventional beam and spatial elements implemented in the commercial FEM program (ANSYS).

The new non-linear bar element of stiffness variability eliminates the disadvantages of conventional beam elements, in which, in case of requirements, it is necessary to include into the solution the variability of section and material properties, to use the "mean" values of these parameters what increases a deviation from the exact solution. Another possibility of taking into account the variability of geometry and material

properties, is the replacement of real bar by sufficient mesh of beam elements, and thus in a graded manner to define longitudinal stiffness variation, what expects increased requirements for the preparation and the time of the problem solution.

The presented results of loading in the elastic area show better agreement of the solution with one new bar element with the results obtained by spatial model SOLID, in comparison with results from comparative models with beam elements BEAM in the commercial software ANSYS. The difference of maximum axial forces for all the considered variations of stiffness calculated by a new element compared to the spatial model is about 3%, and, with increasing degree of the stiffness variability, it decreases. It can therefore be concluded that the results obtained by one new bar element are in good agreement with the results specified by the spatial model. Stiffness matrices of the new non-linear bar element allow to accurately take into account the longitudinal variability of cross section and material properties as a way to create a model "*1 bar = 1 element*". The accuracy of the solution thus depends on the mesh density.

In the next part of the study, the solution of nonlinear problems with new bar element was extended to the area elasto-plastic deformations. Non-linear stiffness matrices for non-incremental problem solving with considering material with bilinear model and isotropic or kinematic hardening were prepared. By numerical experiments, the accuracy of non-linear bar element in dependence on the degree of the polynomial variability of stiffness and the ratio of the maximum and minimum value of stiffness in

the bar was investigated. In solving the problems of deformation in the Von Mises structure in elasto-plastic area by one our bar element of variable stiffness, the results are in better agreement with the solutions obtained from the models with a large number elements (BEAM SOLID) than those obtained from the models with one beam element (BEAM23, BEAM188).
Significant differences in the course of axial forces or reactions occur only in the area of transition from elastic to elasto-plastic state.
This deviation, which occurs in all models with one element (new bar element BEAM23, BEAM188), and is more pronounced when considering the material with kinematic hardening, is caused mainly due to the fact that in the models with a larger number of elements, the transition to elasto-plastic state is made gradually. With a further increase in load, however, the difference between the course of axial forces determined by one new bar element and models decreases. The good agreement occurs in cases where a ratio of the maximum and minimum stiffness of the bar is not greater than 3.0. If the ratio of the extreme values of stiffness in the bar is higher (particularly in the case of considering material with kinematic hardening), the use of a new non-linear bar of variable stiffness to solve the problems with deformations in elasto-plastic area appears to be less accurate, and therefore it is advisable to choose for the solution of such problems a different approach.
Another area in which it is possible to use accuracy and good properties of the new nonlinear bar element are the problems for which the variability of stiffness caused by the use of materials with controlled variability of the material and physical properties such as composite materials, functional

graded materials (FGM) or sandwich structures. In the production of such materials procedures allowing targeted control of variability of material properties by changing individual components of the composite and their reciprocal volume ratios in the volume of the body are used. To assess the stress-strain state of the components made of such materials, it is necessary to determine the variability of homogenized material properties in the body. In general, to determine the homogenized properties of such composite materials, various homogenization techniques are used.

In the commercial FEM programs, modelling of varying material properties can be reduced by using the "mean" value material properties and using fine mesh of finite elements, what causes an increase in the time required to prepare the model and the solution.

In the study, the author used advanced mixing rule designed at the Department of Mechanics (Faculty of Electrical Engineering and Information technology, Slovak University of Technology in Bratislava, Slovakia) allowing, in case of the bar of symmetric constant cross section made from a two-component composite with longitudinal variability of material properties of the components and their volume ratios, to set the varying, effectively homogenized material properties. The homogenized effective modulus of elasticity of the composite material obtained by the designed procedure was then implemented in stiffness matrices of non-linear bar element. The accuracy of the designed mixing rule was compared with an improved mixing rule designed by Love and Batra (36). From the results of the carried out numerical experiment can be concluded, that the differences in the course of axial forces in the bar with homogenized

modulus of elasticity determined by the designed extended mixing rule (MR) and improved mixing rule proposed by Love and Batra (LB) are marginal, and both homogenisation procedures allow to obtain effective homogenized properties of the composite with the same accuracy.

In the next step, a procedure was designed that allows using the extended mixing rule for calculation of the effective homogenized properties of symmetric multilayer sandwich material consisting of layers of composites. Furthermore, the solution was extended by the impact of the inclusion of stationary temperature field represented by a variable longitudinal temperature distribution. All the performed numerical experiments confirmed good agreement of the results of axial forces or reactions, deformations and stresses in the bar, obtained by one non-linear bar element, and the results obtained by the spatial model with dense finite element mesh (SOLID). Solution with one bar element enables a high effective obtaining of the results of deformation and stress distribution in the layers of sandwich bar with accuracy comparable with the results specified by models with spatial or planar elements, and fine mesh at infinitely shorter time of solution. The applied procedure for compiling stiffness matrices of the bar element allows the use of other homogenization techniques for the determination of effective material properties. The only condition is that the resulting relationship describing the variability of material properties in composite layers, as well as the whole composite element, would have the polynomial form.

The second main part is devoted to the derivation of stiffness matrices of non-linear beam element of constant stiffness, determined for the solution

of geometrically non-linear problems with large displacements (rotations) but very small strain. Matrices of the two-noded planar beam element of double symmetric cross section were derived, provided the Euler-Bernoulli conditions for deflection formed by material with linearly elastic property. Matrices of the element were designed from basic geometrically non-linear equilibrium stiffness equation derived from complete geometrically non-linear non-incremental formulation without any linearization of increment GL of the tensor of relative deformation or calculation of the stress tensor increment. As substitute functions at derivation of element stiffness matrices, for axial displacement components and linear polynomials, and for the deflection components of displacement, the cubic hermitian interpolation polynomials were used.

To assess the accuracy and effectiveness of the new nonlinear beam element, the program in MATHEMATICA software was designed. After the necessary modifications, the program was used in the four numerical experiments. As a comparative solution, computational models in ANSYS programme with varying mesh density formed by traditional hermitian beam element BEAM3 and spatial models consisting of the body element SOLID185 were used. The outcomes of the performed numerical experiments with a statically determinate beam showed, that the deformations obtained by one new element are in better agreement with the results obtained from the spatial model consisting of a mesh of body elements SOLID, than the results of displacement defined by the model consisting of 100 traditional elements BEAM. The difference in the values of deformation at statically determinate problems, in comparison with the

solution obtained by the spatial model is at the level of 6%. In solution of statically indeterminate problems, the experiments showed that the new beam element satisfies exactly both global and local equilibrium conditions. Unlike the new element in the carried out numerical experiment, the traditional hermitian beam element satisfied equilibrium equations at the mesh density with 20 elements. From the experiments, it can be concluded that to achieve comparable results, it is necessary to use a model with approximately 3-fold greater number of traditional beam elements than for the model with new beam elements.

Differences in the results of deformations specified by beam models and body elements of spatial stress state was possible to expect mainly due to incomplete agreement of both physical FEM models.

Acknowledgements

This work was supported by the Slovak Grant Agency, grants VEGA 1/0389/11 and VEGA 1/0534/12. This support is gratefully acknowledged.

REFERENCES

1. ALLEN, D. H., HAISLER, W. E. *A theory for analysis of thermoplastic materials*. Computers & Structures, Vol. 13, p. 129-135, 1981.
2. ALTENBACH, H., ALTENBACH, J., KISSING, W. *Mechanics of Composite Structural Elements*. Engineerig - Monograph, Springer-Verlag, 2003.
3. ANSYS 11.0 – Theory manual. SAS IP, 2008.
4. AUGARDE, C. E. *Generation of shape functions for straight beam elements*. Computers & Structures, Vol. 68(6), p. 555, 1998.
5. BATHE, K. J.: *Finite element procedures in engineering analysis*. New Jersey: Prentice-Hall, Inc., 1996.
6. BELÉNDEZ, T., NEIPP, C., BELÉNDEZ, A. *Large and small deflections of cantilever beam*. European Journal of Physics, 23, p. 371-379, 2002.
7. BELÉNDEZ, T., PÉREZ-POLO, M., NEIPP, C., BELÉNDEZ, A. *Numerical and Experimental Analysis of Large Deflections of Cantilever Beams Under a Combined Load*. Physica Scripta, Vol. T118, p. 61-65, 2005.
8. BELYTSCHKO, T., LIU W. K., MORAN B. *Nonlinear Finite Elements for Continua and Structures*. John Wiley and Sons, Chichester, 2001.
9. BENČA, Š.: *Aplikovaná pružnosť I – Metóda konečných prvkov./ Applied elasticity I – Finite element method.* Bratislava: SVŠT, 1987.
10. BENČA, Š.: *Výpočtové postupy MKP pri riešení lineárnych úloh mechaniky. / FEM calculation methods for solving linear problems in mechanics*. Vydavateľstvo STU, Bratislava, 2004.
11. BENČA, Š.: *Riešenie nelineárnych pevnostných úloh pomocou MKP*. / Nonlinear stiffness problem solution using FEM. Nakladateľstvo STU, Bratislava, 2009.
12. BRDIČKA, M., SAMEL, L., SOPKO, B.: *Mechanika kontinua. / Continuum mechanics.* Academia, nakladateľstvo AV ČR, Praha, 2000.
13. CHAKRABORTY, A., GOPALAKRISHNAN, S., REDDY, J. N. *A new beam finite element for the analysis of functionally graded*

materials. International Journal of Mechanical Sciences, Vol. 45 (3), p. 519-539, 2003.
14. CRISFIELD, M. A. *Non-linear finite element analysis of solids and structures, Volume 1*: *Essential*. Chichester: John Wiley & Sons, Inc., 1991.
15. CRISFIELD, M. A.: *Non-linear finite element analysis of solids and structures, Volume 2*: *Advanced topics*. Chichester: John Wiley & Sons, Inc., 1997.
16. ĎURIŠ, R., KUTIŠ, V. *Porovnanie vybraných prístupov k riešeniu geometricky nelineárnych úloh. / Comparison of selected approaches to solving geometrically nonlinear problems*. In: Akademická Dubnica 2004, Dubnica n. Váhom: MtF STU, s. 83-86, 2004.
17. ĎURIŠ, R. *Nonlinear analysis of Mises truss problem and comparison of various nonlinear formulations*. In: Dynamics of Machine Aggregates 2004, Závažná Poruba, MtF STU, 2004.
18. ĎURIŠ, R., MURÍN, J., KUTIŠ, V. *Bar element with varying stiffness for geometric and material non-linearity*. In: Numerical Methods in Continuum Mechanics, NMCM 2005, 10th International conference, Žilina, 2005.
19. ĎURIŠ, R. *A comparison of computing results of a new bar element within Ansys solutions*. In: CO-MAT-TECH 2006, 14. medzinárodná konferencia, STU v Bratislave, s. 224-228, 2006.
20. ĎURIŠ, R. *A nonlinear bar element with varying stiffness*. In: Engineering Mechanics 2006, National Conference with International Participation, Svratka, Institute of Theoretical and Applied Mechanics Academy of Sciences of the Czech Republic, Prague, 2006.
21. ĎURIŠ, R., MURÍN, J. S*andwich Composite Bar Element for Geometric Nonlinear Analysis*. In: Engineering Mechanics 2007, National Conference with International Participation, Svratka, Institute of Theoretical and Applied Mechanics Academy of Sciences of the Czech Republic, Prague, 2007.
22. ĎURIŠ, R., MURÍN, J., KUTIŠ, V. *Nonlinear Composite Truss Finite Element with varying Stiffness*. In: Strojnícky časopis (Journal of Mechanical engineering), Roč. 58, č. 5, s. 273-297, 2007.
23. ĎURIŠ, R., MURÍN, J. *A nonlinear truss finite element with varying stiffness*. In: Applied and Computational Mechanics, Vol. 1, No. 2, s. 417-426, 2007.

24. ĎURIŠ, R., MURÍN, J. *A sandwich bar element for nonlinear thermo-elastic analysis*. In: Applied and Computational Mechanics, Vol. 2, No. 1, s. 25-36, 2008.
25. ĎURIŠ, R. *A Geometric Nonlinear Thermo-elasto-plastic Analysis of a Bar Structure*. In: Machine Modeling and Simulations, Scientific and Technical Society at the University of Žilina, s. 29-36, 2009.
26. FISH, J., CHEN, W., TANG, Y. *Generalized mathematical homogenisation of atomistic media at finite temperatures*. International Journal of Multiscale Computational Engineering, Vol. 3(4), p. 393-413, 2005.
27. HALPIN, J. C., KARDOS, J. L. *The Halpin-Tsai equations. A review*. Polymer Engineering and Science, Vol. 16, No. 5, p. 344-352, 1976.
28. IDESMAN, A. V. *Comparison of different isotropic elastoplastic models at finite strain used in numerical analysis*. Computer methods in applied mechanics and engineering. 192, p. 4659-4674, 2003.
29. KOLÁŘ, V., NĚMEC, I., KANICKÝ, V. *FEM principy a praxe metody konečných prvků. / FEM principles and practice of finite element method*. Praha: Computer press, 1997.
30. KUTIŠ, V. *Nosníkový prvok premenlivého prierezu splňujúci lokálne i globálne podmienky rovnováhy / Beam element of variable cross-section complying both global and local equilibrium conditions*. Doctoral thesis. Bratislava: FEI STU, 2001.
31. KUTIŠ, V., MURÍN, J. *NelinPrut – an internal FEM program*. Department of Mechanics FEI, Slovak University of Technology, Bratislava, 2003.
32. KUTIŠ, V., MURÍN, J. *Stability of a Slender Beam-Columm with Locally Varying Young's Modulus*. Structural Engineering and Mechanics, Vol. 23, No. 1, p. 15-27, 2006.
33. KUTIŠ, V., MURÍN, J. *Stability of a Composite Beam-Column with Transversal and Longitudinal Variation of Material Properties*. In: Proceedings of the 9th International Conference on Computational Structures Technology, Athens, Greece, 2.- 5. September 2008.
34. LEMAITRE, J., CHABOCHE, J. L. *Mechanics of Solid Materials*. Cambridge University press, 1994.
35. LIU, W. K., KARPOV, E. G., PARK, H. S. *Nano Mechanics and Materials: Theory, Multiple Scale Analysis and Applications*, Springer, 2005.

36. LOVE, B. M., BATRA, R. C. *Determination of effective thermomechanical parameters od a mixture of two elastothermoviscoplastic constituents*. International Journal of Plasticity, 22, p. 1026-1061, 2006.
37. MASNÝ, M. *Riešenie viazaných elektro-termo-mechanických úloh s jednorozmerne funkcionálne stupňovaným materiálom metódou konečných prvkov. / Solution of bonded electro-thermo-mechanical problems with one-dimensional functionally graded materials using finite element method.* Doctoral thesis. Department of Mechanics, FEI STU Bratislava, 2001.
38. McGUIRE, W., GALLAGHER, R. H., ZIEMIAN, R. D. *Matrix structural analysis*. New York: John Wiley & Sons Inc., 2000.
39. MELHORN, G.: *Der Ingenieurbau*. Ernst and Sohn, Berlin, 1996.
40. MORI, T., TANAKA, K. *Average stress in matrix and average elastic energy of materials with misfitting inclusions*. Acta Metall. 21, p. 571-574, 1973.
41. MURÍN, J., ÉLESTÖS, P.: *Mechanika kontinua. / Continuum mechanics*. Bratislava: SVŠT, Strojnícka fakulta, 1986.
42. MURÍN, J. *The Formulation of a new non-linear stiffness matrix of a finite element*. Computers and Structures, Vol. 45, No. 5, p. 933-938, 1995.
43. MURÍN, J. *Non-linear equations of a hyperelastic bar and their solution*. Strojnícky časopis, roč. 49, č. 6, s. 373-382, 1998.
44. MURÍN, J., AMINBAGHAI, M. *Vergleichsberechnungen im Rahmen der Th. II. Ordnung mit Programmen IQ-100 and ANSYS*. Proceedings of Strojné inžinierstvo 99, STU Bratislava, 1999.
45. MURÍN, J. *Priestorový nosníkový prvok premenlivého prierezu. / Spatial beam element of variable cross-section*. Inženýrská mechanika, roč. 6, č. 1, s. 25-35, 1999.
46. MURÍN, J. *Nosníkový prvok premenlivého prierezu spĺňajúci globálne i lokálne podmienky rovnováhy. / Beam element of variable cross-section complying both global and local equilibrium conditions*. Strojnícky časopis, roč. 49, č. 3, s. 208-223, 1998.
47. MURÍN, J. *Metóda konečných prvkov pre prútové a rámové konštrukcie. / Finite element method for beam and frame structures*. Bratislava: STU, 1999.

48. MURÍN, J. *Implicit non-incremental FEM equations for non-linear continuum*. Strojnícky časopis, roč. 52, č. 3, s. 147-158, 2001.
49. (1) MURÍN, J., KUTIŠ, V. *Solution of non-incremental FEM equations of non-linear continuum*. Strojnícky časopis, roč. 52, č. 6, s. 360-371, 2001.
50. MURÍN, J., KUTIŠ, V. *3D-beam element with continuous variation of the cross-sectional area*. Computers and Structures, Vol. 80, p. 329-338, 2002.
51. MURÍN, J., KUTIŠ, V. *Beam element with varying stiffness*. Strojnícky časopis, roč. 54, č. 4, s. 239-252, 2003.
52. MURÍN, J., KUTIŠ, V., MASNÝ, M. *Link Element with Variation of Thermal Conduction for Thermal Analysis*. Strojnícky časopis, roč. 56, č. 3, 2005.
53. MURÍN, J., KUTIŠ, V. *Geometrically non-linear truss element with varying stiffness*. Engineering Mechanics, Vol. 13, No. 6, p. 435-452, 2006.
54. MURÍN, J., KUTIŠ, V. *Improved mixture rules for the composite (FGM's) sandwich beam finite element*. AT&P Journal Plus, 1, s. 13-17, 2007.
55. MURÍN, J., KUTIŠ, V. C*omposite beam finite element with variation of Young´s modulus in two direction*. In: IX International Conference on Computational Plasticity COMPLAS IX, Fundamentational and Applications. Part 2., E. Onate and D. R. J. Owen (Eds.), CIMNE, Barcelona, p. 647-650, 2007.
56. MURÍN, J., KUTIŠ, V., MASNÝ, M. *An effective multiphysical FGM's beam/link finite element with transversal symmetric and longitudinal continuous variation of material properties*. In: Proceedings of the 9th International Conference on Computational Structures Technology Athens, Greece, 2.- 5. September 2008.
57. MURÍN, J., KUTIŠ, V., MASNÝ, M. *An effective solution of electro-thermo-structural problem of uni-axially graded material*. Structural Engineering and Mechanics, 28 (6), p. 695-714, 2008.
58. MURÍN, J., KUTIŠ, V., MASNÝ, M., ĎURIŠ, R. *Composite (FGMs) beam finite elements*. In: Kompiš, V., Composites with micro- and nano-structures: Computational Modeling and Experiments, New York, Springer Science and Business Media B.V., 2008.

59. MURÍN, J., KUTIŠ, V. *An effective solution of the composite (FGM's) beam structures*. Engineering Mechanics, Vol. 15, No. 2, p. 115-132, 2008.
60. MURÍN, J., KUTIŠ, V. *An Effective Multilayered Sandwich Beam-Link Finite Element for Solution of the Electro-Thermo-Structural Problems*. Computers and Structures, Vol. 87, 2009.
61. MURÍN, J., AMINBAGHAI, M., KUTIŠ, V. *Exact Solution of the Bending Vibration Problem of FGM Multilayered Sandwich Beam with Variation of Material Properties*. In: COMPDYN 2009. In: 2nd International Conference on Computational Methods in Structural Dynamics and EarthQuake Engineering, Rhodos, Greece, 22.-24.6.2009.
62. NANAKORN, P., VU, L. N. *A 2D field-consistent beam element for large displacement analysis using the total Lagrange formulation*. Finite Elements in Analysis and design, 42, p. 1240-1247, 2006.
63. PSOTNÝ, M. *Stabilné a nestabilné vetvy v riešení geometricky nelineárnych úloh. / Stable and Unstable Paths in the Solution of Geometrically Nonlinear Problems.* Doctoral thesis. Edícia vedeckých prác, STU v Bratislave, Stavebná fakulta, Bratislava, 2004.
64. RAVINGER, J. *Programy. Statika, stabilita a dynamika stavebných konštrukcií. / Programs. Statics, dynamics and stability of building structures*. Bratislava, ALFA, 1990.
65. RAVINGER, J., PSOTNÝ, M. *Von-Misses Truss with Imperfection*. Slovak Journal of Civil Engineering. Vol.XI, No. 2, p. 1-7, 2003.
66. RAVINGER, J., PSOTNÝ, M. *Analýza konštrukcií. Nelineárne úlohy. / Analysis of the structures. Non-linear tasks*. Vydavateľstvo STU Bratislava, 2007.
67. REKTORYS, K. *Přehled užité matematiky. / Overview of Applied Mathematics*. SNTL, Praha, 1963.
68. RUBIN, H., SCHNEIDER, K. J. *Baustatik*. Düsseldorf: Werner Verlag, 1996.
69. RUBIN, H. *Analytische lösung linearer differentialgleichungen mit veränderlichen koeffizienten und baustatische anwendung*. Bautechnik, Vol. 76, 1999.
70. SANKAR, B. V. *An elasticity solution for functionally graded beams*. Composites Science and Technology, 61, p. 689, 2001.

71. SAPOUNTZAKIS, E. J., MOKOS, V. G. *3D-beam element of variable composite cross-section including warping and shear deformation effect*. Computers and Structures, Vol. 85 (1-2), p. 102-116, 2007
72. SHIOTA, I., MIYAMOTO, Y. *Functionally Graded Materials 1996*, Elsevier, 1997.
73. SIMO, J. C., HUGHES, T. J. R. *Computational Inelasticity*. Springer, 2004.
74. TIMOSHENKO, S. P., GERE, J. M. *Theory of Elastic Stability*. McGraw Hill, London, 1961.
75. VASILIEV, V.V., MOROZOV, E.V. *Mechanics and Analysis of Composite Materials*. Elsevier, 2001.
76. WOLFRAM, S. *The MATHEMATICA Book. 5th ed*. WolframMedia, 2003.
77. ZHONG, Z., YU, T. *Analytical solution of a cantilever functionally graded beam*. Composites Science and Technology, 67, 2007.
78. ZIENKIEWICZ, O. C., TAYLOR, R. L. *The finite element method.* London: McGraw-Hill Book Company, 1989.

CONTENTS